BULLETIN OF MARINE SCIENCE, 51(3): 360–406, 1992

LARVAL DEVELOPMENT OF SARGO (*ANISOTREMUS DAVIDSONII*) AND SALEMA (*XENISTIUS CALIFORNIENSIS*) (PISCES: HAEMULIDAE) FROM THE SOUTHERN CALIFORNIA BIGHT

William Watson and H. J. Walker, Jr.

ABSTRACT

Size series of 116 *Anisotremus davidsonii* (2.2–24.9 mm) and 131 *Xenistius californiensis* (2.2–41.7 mm) from field collections were examined for pigmentation, and most specimens were measured to determine morphometric characteristics. Subsets of 39 *A. davidsonii* (2.9–23.6 mm) and 25 *X. californiensis* (2.7–24.1 mm) were cleared and stained to examine skeletal development. Pigment in both species is largely limited to the ventrum and to the dorsal surface of the gut and swimbladder throughout larval development. Both species subsequently develop rather heavy dorsal and dorsolateral pigment; small juveniles display the longitudinal stripes that are well known in juvenile Haemulinae. Both species are moderately slender, with preanal length roughly half of body length. Development in both is gradual, with no marked changes in proportions. Both look like typical haemulines. Skeletal development differs little from that described for other haemulines. Bones of the jaws, operculum, and suspensorium are among the first to ossify, usually before notochord flexion. Ossification of neural and haemal arches and spines and vertebral centra, except the urostyle, is anterior to posterior. Pterygiophores and soft rays form first in the middle of the dorsal and anal fins in both species; addition is both anterior and posterior. Addition of dorsal spines begins posteriorly, but then may continue from anterior to posterior. Larval sargo and salema are distinguished from similar larvae off California and northern Baja California primarily by a combination of myomere count and ventral pigment on the tail. Larval sargo typically have pigment on the peritoneum just anterior to the liver, while larval salema do not. Larval salema usually have a melanophore under the anterior hindbrain, while preflexion stage larval sargo usually do not. After notochord flexion sargo are deeper-bodied than salema. Dorsal fin ray counts allow easy separation of postflexion and older sargo (14–15) from salema (12–13).

In California waters the percoid family Haemulidae is represented by two species: *Anisotremus davidsonii,* the sargo, and *Xenistius californiensis,* the salema. Sargo ranges from the Gulf of California to Santa Cruz Island off southern California, while salema ranges from Peru to Monterey, California (Feder et al., 1974; Miller and Lea, 1972). Sargo was successfully introduced to the Salton Sea in 1951 (Walker et al., 1961). Both species are common in the nearshore Southern California Bight, where the sargo is a highly regarded sport fish. The smaller salema is of minor value as a sport species. The larvae of both species occur during summer in the Southern California Bight where they are essentially restricted to the shallow continental shelf (Ambrose et al., 1988; Sandknop et al., 1988; Stevens et al., 1990; Walker et al., 1987). Feder et al. (1974) noted that juveniles appear close to shore in late summer, in depths of 2–5 m.

Published accounts of larval development are lacking for both species although a postflexion salema was illustrated by Johnson (1984). The species were not distinguished from one another prior to this study (originally presented, in part, at the 1982 California Cooperative Oceanic Fisheries Investigations annual conference, Idyllwild, California, October 1982): both typically were identified as sargo.

In this paper we describe the larval development of sargo and salema, including skeletal development, to facilitate identification of these species in ichthyoplank-

ton samples and as a potential aid in studies of percoid systematics (Johnson, 1984).

Materials and Methods

Larvae, collected near San Onofre, California (ca. 75 km northwest of San Diego) (Barnett et al., 1984), were sorted from 5–10% seawater-Formalin fixed plankton samples, and transferred to sodium-borate buffered 2.5% seawater-Formalin. Juveniles were collected by dipnet near San Diego, California, fixed in Formalin, and stored in 50% isopropanol. The juveniles and all illustrated specimens are stored in the Scripps Institution of Oceanography Marine Vertebrates Collection (SIO); all others are stored at the National Marine Fisheries Service, Southwest Fisheries Science Center, La Jolla Laboratory.

Specimens were examined under a binocular dissecting microscope equipped with an ocular micrometer. Counts and measurements (to the nearest 0.1 mm) were made on the left side. The following dimensions were recorded for each specimen: standard length, total length, pre-anus length, body depth at pectoral fin insertion, eye diameter, snout length, pre-dorsal fin length, pre-anal fin length, and length of longest preopercular spine (dimensions defined by Potthoff et al., 1984; Saksena and Richards, 1975; Stevens and Moser, 1982). Larval lengths refer to standard length unless otherwise specified. Drawings were made with the aid of a camera lucida.

Descriptions are based on the larvae of 111 sargo and 124 salema, and on 5 sargo and 7 salema juveniles. Representative series of 39 sargo and 25 salema were cleared and stained with alcian blue and alizarin red-S, following the method described by Potthoff (1984).

Description of Larvae

Anisotremus davidsonii

Pigmentation (Figs. 1–4).—Pigmentation of sargo is largely restricted to the isthmus, gut and swimbladder, and ventral margin of the tail through most of larval development. During the preflexion stage 10–23 melanophores (mode = 16–17), usually of uniform size, are evenly-spaced along the ventral margin of the tail, beginning at the first or second postanal myomere (a melanophore just above the hindgut, at the last pre-anal myomere, is present in 30% of preflexion specimens <4.5 mm, but is absent thereafter). The number of ventral tail melanophores decreases during notochord flexion to 10–17 (mode = 14) but subsequently changes little (mode = 13–14 during postflexion, 12 during the early juvenile stage). The ventral tail melanophores begin to extend internally during the late preflexion stage; the first 1–4 (usually 1 or 2) become entirely internal and disappear soon after the beginning of notochord flexion. As the anal fin develops (beginning at ca. 4.4 mm), 4 to 7 melanophores move ventrad onto the anal ray bases. The last melanophore along the anal fin base frequently is embedded above the last ray in larvae and the more posterior melanophores also become embedded in juveniles. The anal fin is unpigmented except for the melanophores along the ray bases.

During the preflexion stage 0–5 (mode = 1) small melanophores occur ventrally along the posterior end of the notochord. These melanophores become situated at the bases of developing principal caudal fin rays, usually at one or more of the lower five rays. In late larvae, additional caudal fin melanophores develop along some of the lower principal rays (ca. 12.6 mm), and during the early juvenile stage melanophores develop along some of the upper principal rays (ca. 17 mm). Between 17.2 and 24.9 mm a stripe along the lateral midline of the body extends onto the caudal fin.

Little external pigment develops on the dorsal or lateral surfaces of the trunk or tail, except over the gut area in larvae larger than ca. 8 mm. Near the end of the larval stage (ca. 12.6 mm) a few small melanophores appear along the dorsal margin just anterior to the dorsal fin (Fig. 3b). During the early juvenile stage

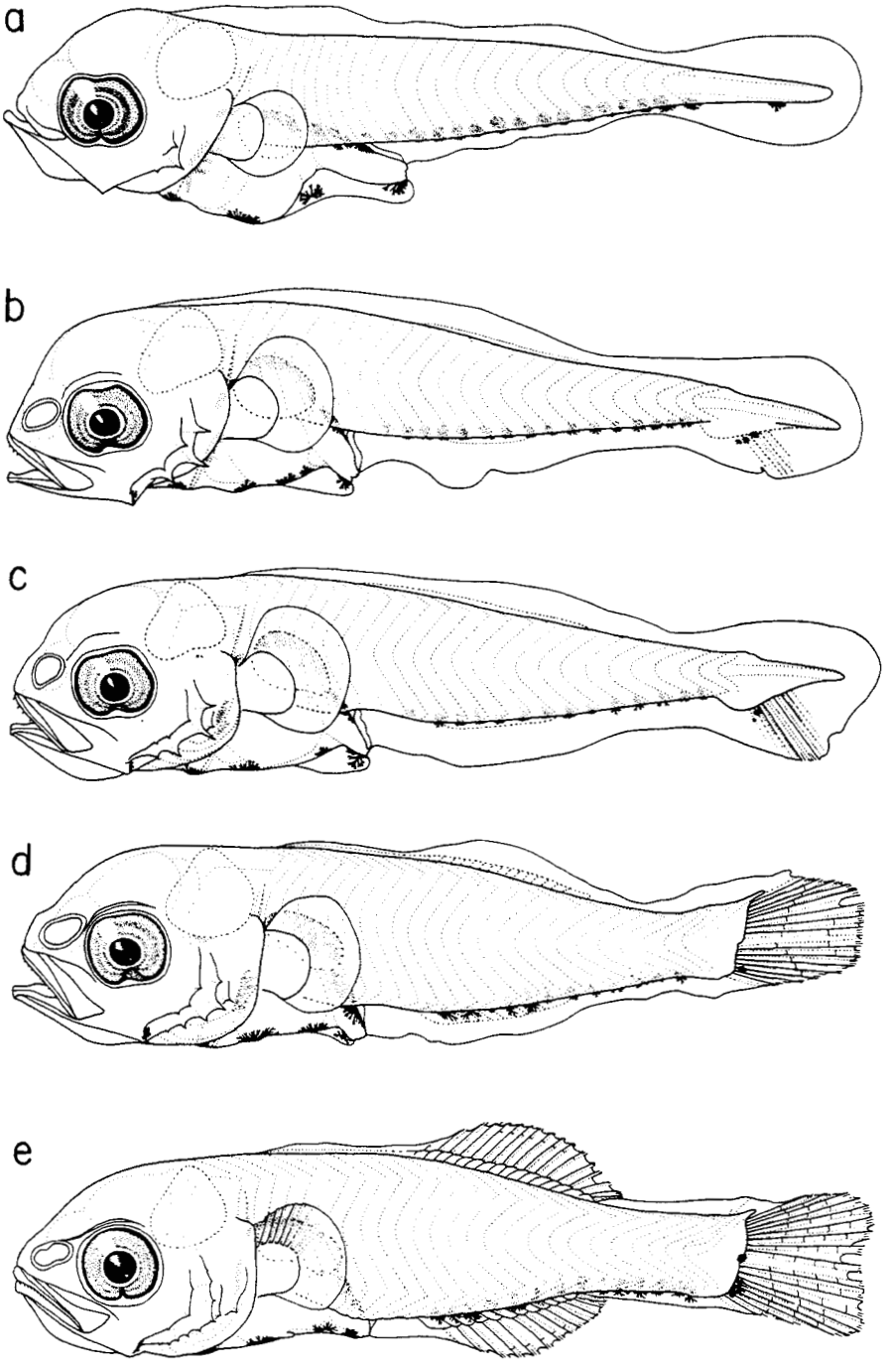

Figure 1. Larval sargo, *Anisotremus davidsonii* (all SIO 91-135): a. 3.0 mm; b. 4.1 mm; c. 4.9 mm; d. 5.2 mm; e. 7.2 mm.

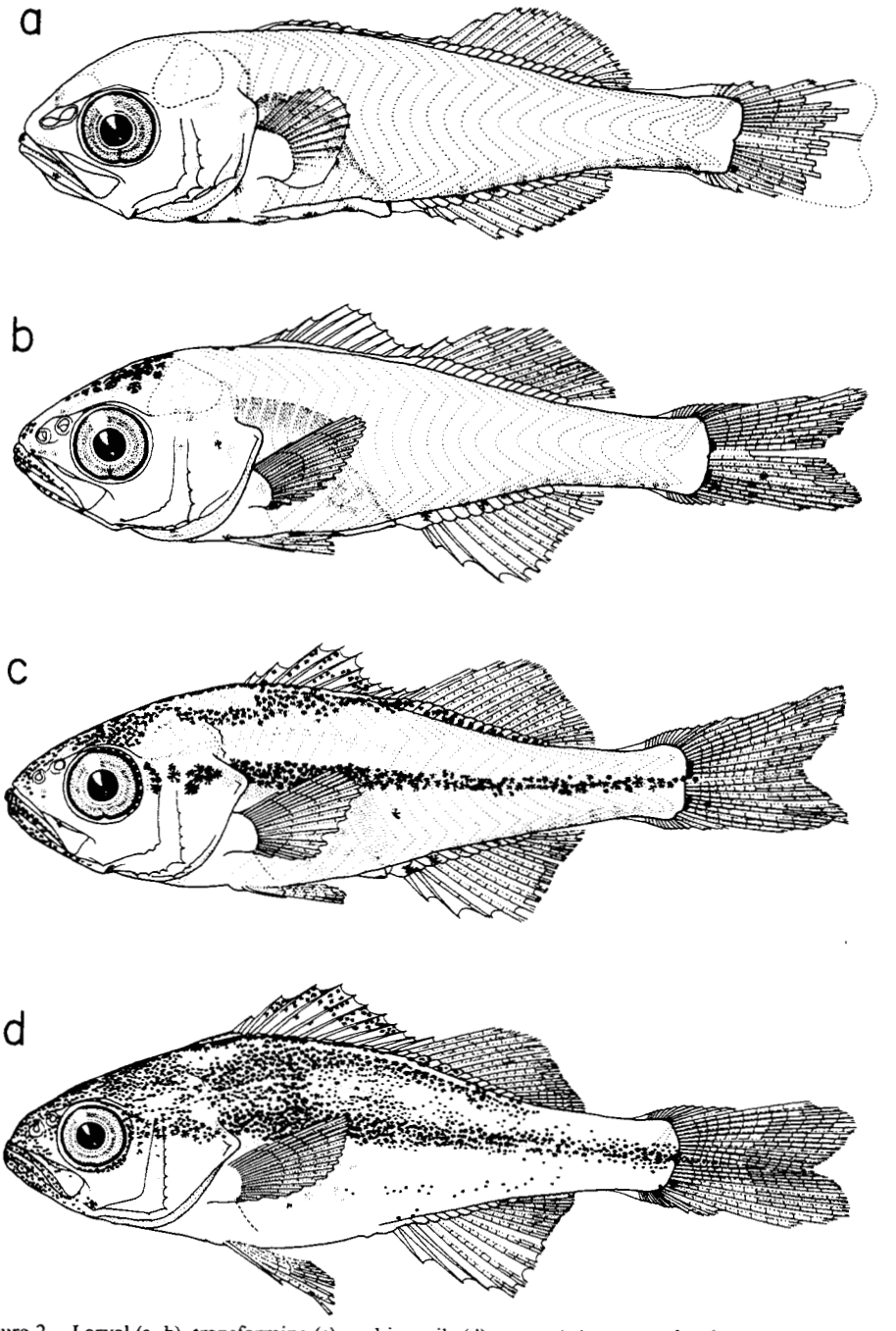

Figure 2. Larval (a, b), transforming (c), and juvenile (d) sargo, *Anisotremus davidsonii*: a. 8.5 mm (SIO 91-135); b. 12.6 mm (SIO 64-249); c. 17.2 mm (SIO 64-249); d. 24.9 mm (SIO 62-346).

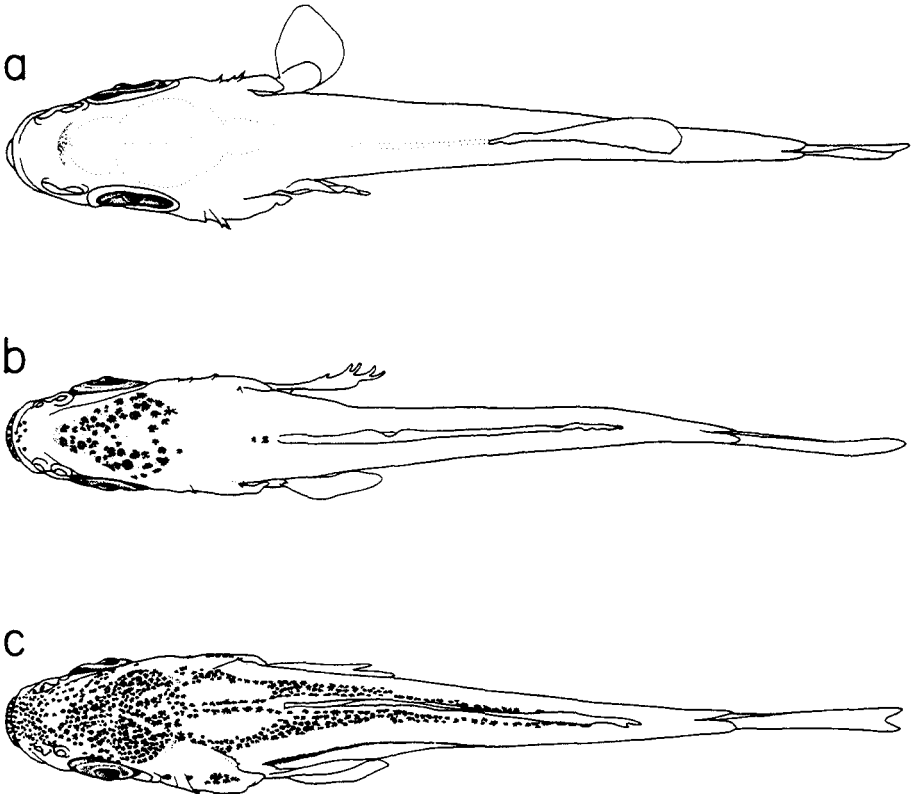

Figure 3. Larval (a, b) and transforming (c) sargo, *Anisotremus davidsonii*, in dorsal view: a. 8.5 mm (SIO 91-135); b. 12.6 mm (SIO 64-249); c. 17.2 mm (SIO 64-249).

dorsal pigmentation increases rapidly: by 17.2 mm pigmentation is continuous along the dorsal margin to the dorsal fin insertion (Fig. 3c), extending up along the dorsal fin ray bases and onto the membranes between most of the dorsal fin spines (Fig. 2c). In addition, by ca. 17 mm a diagonal band of melanophores extends from the otic region to the middle of the spinous dorsal fin, and a stripe extends along the lateral midline to the end of the peduncle (Fig. 2c). The diagonal band subsequently broadens and extends posteriorly, and together with melanophores proliferating upward from the lateral midline, covers most of the upper half of the trunk and tail to the last dorsal ray by ca. 25 mm (Fig. 2d).

External pigment over the lateral gut region develops in the postflexion stage (Fig. 2a). This initially (ca. 8.2 mm) consists of a single melanophore just below the lateral midline at the level of the posterior end of the swimbladder. Melanophores subsequently are added over the entire lateral surface of the abdomen. A few ventrolateral tail melanophores, more-or-less continuous with the external gut pigment, develop during the early juvenile stage (Fig. 2c, d).

The gut is always pigmented dorsally (including pigment over the swimbladder), anteriorly, and externally along the ventral midline. During the preflexion stage dorsal gut pigment consists of one melanophore just anterior to the swimbladder (present in 89%), pigment on the dorsum (87%) or dorsum and posterior surface

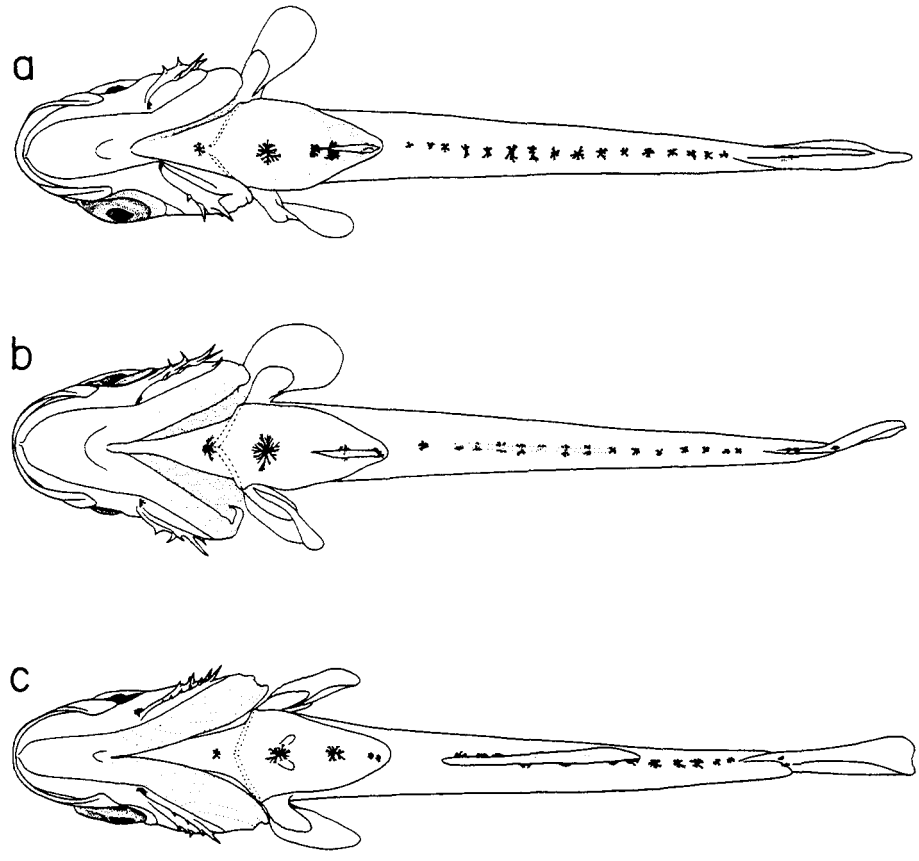

Figure 4. Larval sargo, *Anisotremus davidsonii*, in ventral view (all SIO 91-135): a. 4.1 mm; b. 4.9 mm; c. 7.2 mm.

(13%) of the swimbladder, and one to four (mode = 1) melanophores dorsally on the hindgut. Pigment spreads downward over the dorsolateral surfaces of the swimbladder during notochord flexion. The pigment on the dorsal surface of the hindgut extends anteriorly to the swimbladder and posteriorly to near the anus during flexion and postflexion stages. Pigment nearly always is present anteriorly adjacent to the liver (present in 87% of preflexion, 95% of flexion, and 100% of postflexion stage specimens); this typically is a single large melanophore.

Ventral pigment on the gut consists of one to six external melanophores (mode = 3) about evenly-spaced along the midline from the anterior midgut to the posterior hindgut. The midgut pigment always is present but about 25% of the specimens lacked the hindgut pigment. When pelvic fins develop, the first melanophore in this ventral series lies at the pelvic base.

Internal lateral pigment begins to develop over the dorsolateral gut region at ca. 8.2 mm. This pigmentation rapidly proliferates, so that by the end of larval development scattered internal melanophores cover nearly the entire gut area.

Head pigmentation during the preflexion and flexion stages is largely restricted to a melanophore under the hindbrain, one at each angular, and one on the isthmus

Table 1. Summary of measurements (in mm) of *Anisotremus davidsonii*. Body lengths are notochord length for preflexion and flexion-stage larvae, and standard length for postflexion and juvenile specimens. Measurements of body parts are summarized over 1 mm size classes; for each summary the mean measurement ($\bar{x}$), standard deviation (SD) and number of specimens measured (N) is given. Most specimens between dashed lines are undergoing notochord flexion (actual range undergoing flexion is 4.2–6.0 mm); specimens below the dotted line are juveniles

Body length	Snout length			Eye diameter			Head length			Pre-Anus length			Pre-Dorsal fin length			Pre-Anal fin length			Body depth			Longest pre-opercular spine		
(mm)	$\bar{x}$	SD	N	$\bar{x}$	SD	N	$\bar{x}$	SD	N	$\bar{x}$	SD	N	$\bar{x}$	SD	N	$\bar{x}$	SD	N	$\bar{x}$	SD	N	$\bar{x}$	SD	N
2.0–2.9	0.1	0.04	8	0.3	0.03	9	0.7	0.1	9	1.2	0.1	9							0.6	0.1	9	0.03	0.03	8
3.0–3.9	0.2	0.1	27	0.3	0.04	27	0.9	0.1	27	1.5	0.2	27							0.8	0.1	27	0.1	0.02	27
4.0–4.9	0.3	0.1	25	0.4	0.04	25	1.2	0.1	25	1.9	0.2	25	2.2	0.2	6	2.3	0.2	16	1.0	0.1	25	0.1	0.01	25
5.0–5.9	0.5	0.1	12	0.6	0.04	12	1.7	0.2	12	2.6	0.3	12	2.5	0.4	8	2.9	0.2	7	1.4	0.1	12	0.1	0.01	12
6.0–6.9	0.6	0.1	14	0.7	0.04	14	2.1	0.2	14	3.2	0.1	14	2.4	0.2	14	3.5	0.1	7	1.7	0.1	14	0.1	0.02	14
7.0–7.9	0.7	0.03	10	0.7	0.04	10	2.3	0.2	10	3.5	0.2	10	2.6	0.1	10	3.9	0.2	7	1.8	0.1	10	0.1	0.02	10
8.0–8.9	0.8	0	2	0.8	0.1	2	2.7	0	2	4.2	0.1	2	2.9	0.03	2	4.5	—	1	2.2	0.1	2	0.1	0.01	2
9.0–9.9	0.7	—	1	0.7	—	1	3.0	—	1	4.3	—	1	3.4	—	1	4.5	—	1	1.8	—	1	0.1	—	1
12.0–12.9	1.2	—	1	1.2	—	1	4.5	—	1	6.9	—	1	4.5	—	1	6.9	—	1	3.4	—	1	0.1	—	1
17.0–17.9	1.7	0.1	3	1.8	0	3	6.1	0.2	3	9.6	0.2	3	6.2	0.3	3	9.8	0.3	3	5.3	0.04	3	0.1	0.02	3
19.0–19.9	1.7	0.1	2	1.8	0.1	2	6.6	0.3	2	10.8	0	2	6.8	0	2	11.2	0.1	2	5.7	0	2	0.04	0.06	2

near the cleithral symphysis (present in 69% of preflexion, 97% of flexion, and all postflexion stage specimens). Apart from the isthmus melanophore, head pigment is entirely lacking in specimens smaller than 3.3 mm, and is present under the hindbrain in 7% and on the angular in 30% of the remaining preflexion stage specimens. The ventral hindbrain and angular pigment are present in 81% and 100%, respectively, of flexion and postflexion stage specimens.

An internal melanophore at the anterior margin of the forebrain, developing as early as ca. 6.4 mm, is present in 18% of postflexion specimens smaller than 7.2 mm and in 100% of larger larvae. One or two smaller melanophores may develop along the anterior margin of the forebrain, beginning at ca. 8.2 mm. External pigment may develop over the forebrain as early as 7.8 mm, but usually is absent in specimens smaller than ca. 9 mm. External pigment becomes dense over the fore- and midbrain region by ca. 12.6 mm and extends both anteriorly and posteriorly to completely cover the top of the head by 17.2 mm. This pigment is continuous dorsally with both the dorsal margin pigment and the anterior diagonal band, and ventrally with anterior premaxillary, dentary, and gular pigment.

Internal pigment may develop along the anterior sides of the hindbrain as early as 8.2 mm, but usually is absent until after ca. 9 mm. The hindbrain pigment becomes rather dense early in the juvenile stage, spreading onto the posterior region of the midbrain by 17.2 mm and nearly surrounding the brain in larger specimens.

Morphology.—The smallest sargo larva examined (2.2 mm) showed no evidence of yolk or oil droplet. At this size the eye is pigmented, the mouth is functional, the swimbladder is inflated, and the gut is tubular and folded into a broad "S" shape. The fold tightens, forming a coil in the midgut between 2.9 and 3.2 mm. Notochord flexion begins between 4.2 and 4.7 mm and is completed between 6.0 and 6.2 mm. Transformation to the juvenile stage (indicated by scale formation, which is anterior to posterior) begins at ca. 14–15 mm and is complete by ca. 19–22 mm.

Larval development is a gradual process with no marked changes in body proportions (Figs. 1, 2; Table 1). Snout length, head length, pre-anus length, and body depth all increase slightly relative to standard length (SL) during larval life. Snout length averages 7% of SL (range 4–9%) during the preflexion stage, increases to 9% (range 7–10%) during notochord flexion and to 10% (range 8–13%) in the postflexion stage. Mean proportions (and ranges) for head length are: preflexion stage 27% (22–31%), flexion stage 30% (26–34%), and postflexion stage 33% (28–36%). Respective values for pre-anus length are 45% (41–51%), 46% (37–50%), and 49% (46–55%); and for body depth 24% (19–26%), 25% (20–29%) and 26% (24–28%). Pre-dorsal fin length decreases as the fin develops, from 47% (range 36–53%) of SL during notochord flexion to 36% (range 33–39%) in postflexion larvae. Pre-anal fin length, on the other hand, remains 53% of SL (range 50–60% during notochord flexion, 51–56% following flexion). Eye diameter likewise remains 10% of SL (range 8–11% over all stages) throughout larval development.

Skeletal Development.—Skeletal development of sargo closely resembles that of *Anisotremus virginicus,* described by Potthoff et al. (1984). Since Potthoff et al. (1984) provided good descriptions of development of the hyoid and branchial arches and axial skeleton of *A. virginicus,* descriptions of these in sargo are limited to figures, tables, listings of the few differences from *A. virginicus,* and in some cases, brief supplemental descriptions. Development of the neurocranium, jaws,

Table 2. Summary of skeletal development of *Anisotremus davidsonii*: size (mm SL) of smallest cleared and stained specimen with given structure visible as cartilage, or beginning to ossify; D = dermal origin

Structure	Size at first appearance of	
	Cartilage	Ossification
Neurocranium		
Basioccipital		4.2
Exoccipital		4.2
Parasphenotic		3.5
Pterosphenotic		8.7
Basisphenotic		14.9
Vomer		6.6
Lateral ethmoid		5.5
Median ethmoid	D	12.4
Lachrymal	D	7.1
Circumorbital 2	D	14.9
3	D	12.4
4	D	12.4
5	D	12.4
Dermosphenotic	D	14.9
Frontal	D	5.0
Parietal	D	6.6
Supraoccipital	D	6.6
Sphenotic		6.6
Pterotic		5.4
Prootic		4.5
Epiotic		5.5
Nasal	D	8.7
Jaws and suspensorium		
Premaxillary		2.9
Maxillary		2.9
Dentary		2.9
Articular	2.9	3.9
Angular	2.9	3.9
Hyomandibular	2.9	4.2
Symplectic	2.9	4.2
Quadrate	3.5	4.2
Ectopterygoid	4.2	4.6
Mesopterygoid	4.2	4.2
Metapterygoid	4.2	8.4
Palatine	4.6	5.7
Opercular series		
Preopercular	D	2.9
Opercular	D	2.9
Subopercular	D	4.2
Interopercular	D	4.2
Hyoid arch		
Branchiostegal	D	4.2
Ceratohyal	2.9	4.2
Epihyal	2.9	4.2
Interhyal	3.5	4.2
Ventral hypohyal	3.5	4.6
Dorsal hypohyal	3.5	5.7
Urohyal	D	4.2
Basihyal	5.4	8.7
Branchial arches		
Ceratobranchial	2.9	4.2
Epibranchial	3.5	4.2

Table 2. Continued

Structure	Size at first appearance of	
	Cartilage	Ossification
Hypobranchial	4.2	5.5
Basibranchial	3.5	5.5
Pharyngobranchial	3.5	5.7
Axial skeleton		
Vertebral centra		4.5
Urostyle		5.5
Neural arches	4.2	4.7
Haemal arches	4.2	4.7
Neural spines	4.2	5.7
Haemal spines	4.2	12.4
Epipleural ribs	D	12.1
Pleural ribs	8.7	12.1
Epurals	4.7	12.4
Hypurals 1–4	4.2	5.5
Hypural 5	7.1	8.7
Parhypural	4.2	7.1
Uroneurals		12.4
Caudal distal radials	12.9	
Dorsal pterygiophores	5.7	
Proximal radials	7.1	8.7
Distal radials	7.1	8.7
Anal pterygiophores	5.7	
Proximal radials	7.1	8.7
Distal radials	7.1	8.7
Pectoral and pelvic girdle		
Cleithrum		2.9
Supracleithrum	D	4.5
Dorsal postcleithrum	D	5.5
Ventral postcleithrum	D	4.7
Posttemporal	D	4.5
Supratemporals	D	12.4
Scapula	4.2	7.1
Coracoid	4.2	5.7
Pectoral proximal radials	6.7	12.4
Pectoral distal radials	14.4	
Basipterygia	8.7	12.4

and suspensorium of sargo are described in more detail, since Potthoff et al. (1984) did not deal with these structures in *A. virginicus*.

Initial ossification of each bone is visible as a very thin, hyaline layer forming on (or in) the corresponding cartilage or other tissue. This ossifying layer stained very lightly or not at all. Thus, a degree of uncertainty (probably ≤ 0.5 mm) should be assumed in the following descriptions of size at the beginning of ossification of each bone.

Neurocranium (Fig. 5, Table 2).—CHONDROCRANIUM. The chondrocranium of the smallest stained specimen (2.9 mm) consists of a small ethmoid plate, anteriorly fused trabeculae cranii, and the anterior and ventral parts of the auditory capsule (including a short anteriorly-directed postorbital process). The ethmoid plate subsequently broadens, and by 4.2 mm a dorsal process, the nasal septum, begins to extend from its anterior surface. Simultaneously, the laminae orbitonasalis begin to extend upward on each side from the lateral margin of the ethmoid plate,

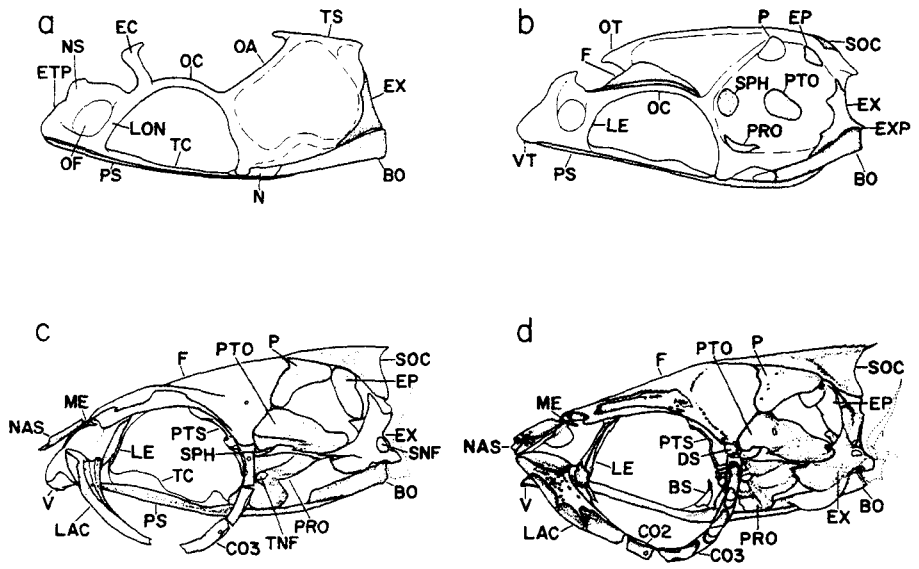

Figure 5. Lateral view of the developing neurocranium of sargo, *Anisotremus davidsonii*: a. 4.2 mm (SIO 91-135); b. 6.7 mm (SIO 91-135); c. 14.9 mm (SIO 91-136); d. 23.6 mm (SIO 62-346). White = cartilage; stippled = ossifying. Abbreviations are: BO = basioccipital; BS = basisphenotic; CO = circumorbitals; DS = dermosphenotic; EC = epiphysial cartilage; EP = epiotic; ETP = ethmoid plate; EX = exoccipital; EXP = posterior exoccipital process; F = frontal; LAC = lacrymal; LE = lateral ethmoid; LON = lamina orbitonasalis; ME = median ethmoid; N = notochord; NAS = nasal; NS = nasal septum; OA = occipital arch; OC = orbital cartilage; OF = olfactory foramen; P = parietal; PRO = prootic; PS = parasphenotic; PTO = pterotic; PTS = pterosphenotic; SNF = foramen of first spinal nerve; SOC = supraoccipital; SPH = sphenotic; TC = trabecula communis; TNF = foramen of trigeminofacialis nerve; TS = synotic tectum; V = vomer; VT = vomerine tooth.

meeting the nasal septum between 4 and 4.5 mm, to define the olfactory foraminae. The orbital cartilages are complete at their first appearance (ca. 4 mm); each is fused anteriorly with the lamina orbitonasalis and posteriorly with the postorbital process of the auditory capsule, which itself is complete by ca. 4 mm. At this same size, the epiphysial cartilage, which bridges dorsally between the orbital cartilages, and the broad synotic tectum, which bridges dorsally between the auditory capsules, first appears in nearly final form. A narrow medial strip of cartilage bridges longitudinally between the epiphysial cartilage and the synotic tectum at ca. 4.6–4.8 mm. The trabeculae cranii are fused and a broad parachordal cartilage is present by ca. 4.5 mm. The chondrocranium apparently changes little subsequently, except that the trabecula communis separates into anterior and posterior parts, after 14.4 mm but before 17.9 mm. By ca. 20 mm the former trabecula consists anteriorly of a very short cartilaginous stub, and posteriorly of a cartilaginous foundation for the basisphenotic.

FRONTAL. The frontals first appear at ca. 5 mm (the frontals were ossifying in a single 4.3 mm specimen, but apparently were not ossifying in the other specimens <5 mm). Initially, each is a small, thin, elongate and somewhat oval dermal ossification above the eye. Subsequently, the frontals expand mesially, posteriorly, and to a lesser extent anteriorly, meeting along their mesial edges by ca. 7–8 mm. A supraocular shelf develops along the exterior edge of each between 6–6.5 mm. This shelf forms a U-shaped trough (open dorsally) during postflexion, and between ca. 14.5 and 20 mm the trough begins to close, from anterior to posterior,

to form part of the supraorbital canal of the laterosensory system. There are no supraocular spines. The frontals are very thin throughout larval development: the chondrocranium is easily seen through the frontals to at least 20 mm.

PARIETAL. Small, thin, oval parietals are first visible in the angle between the auditory capsule and synotic tectum at 6.5–7 mm. Each enlarges, primarily ventrad and slightly caudad, becoming roughly T-shaped by ca. 12.5–14.5 mm. Each parietal abuts against the supraoccipital and adjacent frontal by ca. 8.5–9 mm, abuts against (or slightly overlaps) the adjacent epiotic between ca. 12 and 18 mm, and overlaps the edge of the supraoccipital by ca. 14.5 mm.

BASIOCCIPITAL, EXOCCIPITAL, SUPRAOCCIPITAL. The basioccipital and exoccipital apparently are the second neurocranial elements to begin ossifying, by ca. 4 mm (Table 2). The basioccipital initially is a thin ossification around the notochord. Beginning at ca. 6.5 mm, a pair of very thin flanges extend laterally from its dorsolateral surfaces. Each soon becomes a shallow cup-like structure that forms the lower third of the saccular capsule.

The exoccipitals initially are thin, somewhat crescent-shaped ossifications along the dorsolateral surfaces of the posterior third of the basioccipital, continuing dorsad along the margins of the foramen magnum. Subsequent ossification dorsad and anteriad results in large, complex bones that form most of the posterior neurocranium and encircle all but the floor of the foramen magnum. The lateral wing of each exoccipital forms the roof of the saccular capsule. A posterior process of each exoccipital, first visible at ca. 4.5 mm, articulates with the first vertebral centrum. This process extends to about mid-way along the centrum (reached by ca. 14.5 mm). A thin process arising (ca. 9 mm) from the dorsal margin of the posterior exoccipital process bridges to the posterior margin of the ascending wing of the exoccipital by ca. 12.5–14.5 mm to define the first spinal nerve foramen.

The supraoccipital is first visible at ca. 6.5 mm as a very thin sliver of bone, medially above the posterior half of the synotic tectum. It first lengthens, and a crest begins to form (ca. 8.5–9 mm). The crest becomes triangular and rather large by ca. 14.5 mm, and serrate along its dorsal margin by ca. 20 mm. The supraoccipital expands laterally beginning at ca. 9–12 mm, forming a cap over the posterodorsal neurocranium. The supraoccipital abuts against the frontals at ca. 8.5–9 mm, is slightly overlapped by the parietals by ca. 14.5 mm, abuts against the epiotics by ca. 20 mm, and begins to form an interdigitating joint mesially with the exoccipitals in the largest cleared and stained specimen (23.6 mm).

BASISPHENOTIC, PARASPHENOTIC, PTEROSPHENOTIC, SPHENOTIC. A long, slender parasphenotic ossification, lacking ascending wings, lies along the ventral margin of the ethmoid plate and trabecula communis by ca. 3.5 mm. The ascending wings first appear as short stubs by ca. 4.5 mm, and extend to just below the trigeminofacialis foramen in the prootic by ca. 12.5–14.5 mm. A Y-shaped fork at the posterior end of the parasphenotic extends ventrolaterally on the basioccipital beginning at ca. 4 mm.

The sphenotic is first visible at ca. 6.5 mm as a small, thin, circular ossification just posterior to the junction of the orbital cartilage and auditory capsule. It remains essentially unchanged, until ca. 12.5 mm, when a small, laterally-directed flange develops on its lower surface. This flange first extends diagonally across the lower part of the sphenotic, then develops a short ascending section along the lower anterior sphenotic margin. Finally, the flange grows upward along its distal margin, to form a trough which receives the lower end of the dermosphenotic (ca. 20 mm).

The pterosphenotics begin to ossify by ca. 8.5 mm. Each initially is a thin, slender, crescent-shaped ossification posteriorly along the margin of the orbital

cartilage, and subsequently lengthens and extends posterolaterally to articulate with the frontal, sphenotic, and prootic by ca. 10 mm. The pterosphenotics remain thin and lightly ossified, except in a thin, well-ossified strip along the anterior margin, in the largest specimen stained (23.6 mm).

The basisphenotic begins to ossify at ca. 14.5 mm. It is located medially above the parasphenotic, just anterior to its ascending wings, on a cartilaginous base that apparently is the posterior remnant of the trabecula communis. The basisphenotic does not articulate directly with any other bone in the cleared and stained specimens.

VOMER. The vomer first appears at ca. 6.5 mm as two separate, very thin, slender ossifications on the anterolateral margins of the ethmoid plate. Each ossification is centered around a small vomerine tooth. By ca. 8.5 mm the two vomerine ossifications have joined across the anterior margin of the ethmoid plate, forming a thin, crescent-shaped vomer. Subsequent ossification results in a T-shaped vomer by ca. 12.5 mm; the two vomerine teeth persist to at least 14.4 mm, but are not visible in juveniles (apparently absent by ca. 20 mm).

EPIOTIC, PROOTIC, PTEROTIC. Each of these is first visible between ca. 4.5 and 5.5 mm (Table 2), as a small, thin, oval ossification. The prootic and pterotic apparently begin ossifying slightly before the epiotic. The prootics expand rapidly and substantially, forming much of the floor of the brain case by the end of the larval stage. Each articulates with the sphenotic and pterotic by ca. 8.5 mm, with the exoccipital and ascending wing of the parasphenotic by 12.5–14.5 mm, and is separated from the pterosphenotic only by a thin strip of cartilage by ca. 22.5 mm. The foramen for the trigeminofacialis nerve is a prominent feature from ca. 8.5 mm onward. The pterotic quickly expands, primarily longitudinally, becoming distinctly oval by 6.5 mm. It overlaps the sphenotic by ca. 13 mm and reaches the posterior margin of the frontal by 14.4 mm. A low longitudinal ridge arises from the lateral surface of the pterotic beginning by ca. 13 mm: this is the lower margin of the pterotic canal of the laterosensory system, which is formed by ca. 23.5 mm. The epiotics expand, primarily ventrad, becoming elongate ovals by ca. 8.5 mm and, together with the exoccipitals, form most of the posterior neurocranium by ca. 20 mm. The epiotics abut against the supraoccipital by ca. 13–14.5 mm, overlap the exoccipitals by ca. 20 mm, and are overlapped along their anterodorsal margin by the parietals, at ca. 22.5–23.5 mm.

LATERAL ETHMOID, MEDIAN ETHMOID. The lateral ethmoids begin to ossify between 4.7 mm and ca. 5.5 mm. Each initially appears as a thin, slender ossification along the posterior margin of the lamina orbitonasalis, and subsequently expands dorsally, ventrally, and laterally, to form a shallow U-shaped ossification around the posterior half (approximately) along most of the length of the lamina orbitonasalis, by ca. 12 mm. A mesial flange develops along the lower half of each lateral ethmoid beginning ca. 14.5 mm, but the two mesial flanges remain widely separated in the largest cleared and stained specimen. Each lateral ethmoid reaches the adjacent frontal at about 14.5 mm, and articulates with the adjacent lacrymal by ca. 22.5 mm. A short tube, through which the olfactory nerve passes, develops on the upper anterior surface of the lateral ethmoid at ca. 22.5–23.5 mm.

The median ethmoid first appears at ca. 12.5 mm as a thin, slender ossification along the anterodorsal margin of the nasal septum. Lateral wings begin to develop near its upper end at ca. 13 mm, so that it becomes roughly T-shaped in dorsal view. Subsequent lateral expansion results in the median ethmoid becoming somewhat pear-shaped (in dorsal view), with the lateral wings extending from the narrower upper end. The median ethmoid meets the anterior margins of the frontals by ca. 20 mm.

NASAL. The nasals, which begin to ossify by ca. 8.5 mm, first appear as small, thin, U-shaped dermal bones just above and lateral to the nasal septum. They become larger and somewhat more deeply U-shaped, but otherwise change little through the end of larval development. In early juveniles, each nasal closes dorsally, beginning at the anterior end, to become a tube (ca. 20–22.5 mm) at the anterior end of the laterosensory canal system.

CIRCUMORBITALS. The lacrymal is the first circumorbital bone to develop, beginning between ca. 7–8.5 mm. In the 8.2 mm cleared and stained specimen, it is a flat, somewhat triangular bone, with a narrow lateral flange along its anterolateral edge. This flange expands and grows upward; at ca. 22.5–23.5 mm it meets a second lateral flange that arises (ca. 13–14.5 mm) from the lateral surface of the lacrymal, to form a low, oval tube. Concurrently, the lacrymal enlarges substantially, extending at its dorsal margin (by ca. 22.5 mm) from the level of the posterior margin of the lateral ethmoid to just beyond the anterior end of the ethmoid plate. The upper part of the lacrymal becomes somewhat cup-shaped at its posterior end, where it articulates with the lower end of the lateral ethmoid. Circumorbitals 3–5 apparently begin ossifying more-or-less simultaneously, at ca. 12.5 mm. Each initially is a thin, flat to shallowly U-shaped dermal ossification; by ca. 23.5 mm all are becoming tubular. Circumorbital 2 and the dermosphenotic are the last to form, at ca. 14.5 mm. In the largest cleared and stained specimen, circumorbital 2 is a shallow U-shaped bone, and the dermosphenotic is an essentially flat oval-shaped bone that is inserted along its lower margin into the lower sphenotic.

Jaws and Suspensorium (Fig. 6, Table 2).—MAXILLARY, PREMAXILLARY, ROSTRAL CARTILAGE. In the smallest cleared and stained specimen (2.9 mm) the upper jaw consists of a pair of long, slender maxillaries and a pair of very small, more-or-less triangular premaxillaries, each with a single tooth. The maxillaries quickly broaden, more so distally. Each develops a short anterior process near its anteroventral margin; this process extends laterally to just beyond the posterior margin of the premaxillary by ca. 4 mm. A short dorsal process develops simultaneously at the same level. Both processes subsequently broaden, and the dorsal process forms an inverted "U" whose legs diverge ventrad, with the mesial leg extending to the anteroventral margin of the ethmoid plate by ca. 8.5 mm. A thin, posteriorly-directed flange arising from the interior margin of the ascending process of the premaxillary fits loosely into the inverted U of the maxillary, to form a tongue and groove-like joint by ca. 8.5 mm.

A short ascending process and a long, slender posterior process bearing three teeth develop on each premaxillary by 4.2 mm. The premaxillaries subsequently broaden, with the posterior process of each broadening much more, to form a flat crescent-shaped flange (by ca. 6.5 mm) that extends dorsad, mesial to the maxillary, reaching well past the upper maxillary margin by ca. 20 mm (Fig. 6d).

The rostral cartilage, a large, oval cartilage first visible at ca. 5.5–6.5 mm, lies between the premaxillary ascending processes. The ascending processes reach three-quarters of the way up its length at 6.5 mm, and the posterior premaxillary flanges reach about one-third up each side by ca. 20 mm.

ANGULAR, ARTICULAR, DENTARY. The lower jaw of the smallest cleared and stained specimen consists of the paired Meckel's cartilages, which abut mesially at their anterior ends. A slender dentary ossification bearing two teeth lies along the anterodorsal margin of each. The dentaries soon deepen and extend posteriorly, each forming a Y-shaped articulation with the anterior end of the ossifying articular by ca. 4 mm. The dentary canal of the laterosensory system is first apparent at ca. 8–8.5 mm as a shallow groove along the lower lateral surface on

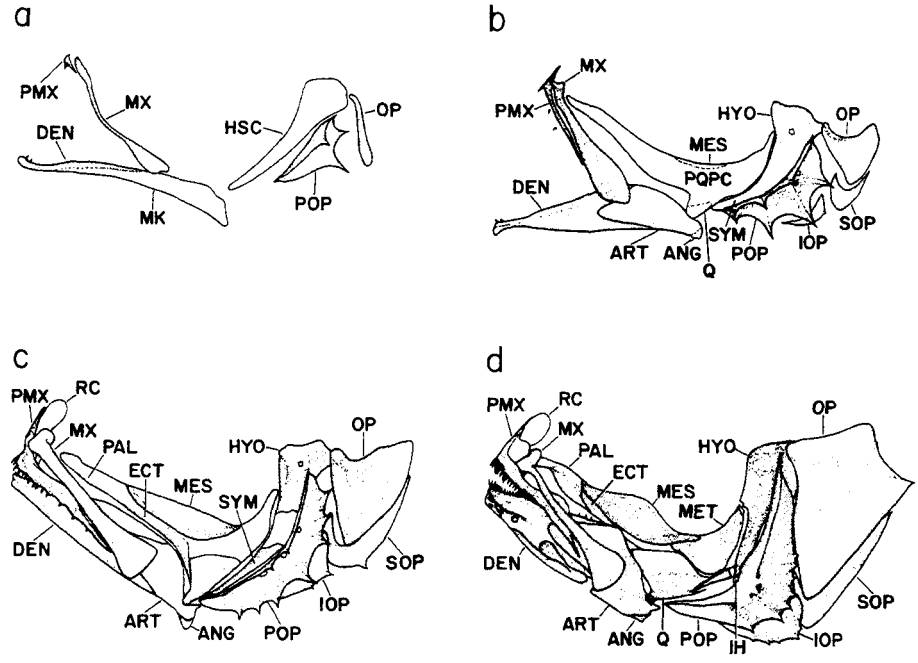

Figure 6. Development of the jaws, suspensorium, and opercular bones of sargo, *Anisotremus davidsonii*: a. 2.9 mm (SIO 91-135); b. 4.2 mm (SIO 91-135); c. 6.7 mm (SIO 91-135); d. 23.6 mm (SIO 62-346). White = cartilage; stippled = ossifying. Abbreviations are: ANG = angular; ART = articular; DEN = dentary; ECT = ectopterygoid; HSC = hyomandibulosymplectic cartilage; HYO = hyomandibular; IOP = interopercular; MES = mesopterygoid; MET = metapterygoid; MK = Meckel's cartilage; MX = maxillary; OP = opercular; PAL = palatine; PMX = premaxillary; POP = preopercular; PQPC = palato-pterygoquadrate cartilage; Q = quadrate; RC = rostral cartilage; SOP = subopercular; SYM = symplectic.

the anterior half of the dentary. This groove closes to form a tube, from anterior to posterior, beginning by ca. 20 mm.

Each articular begins to ossify at ca. 4 mm, along the lower lateral face of the posterior half of Meckel's cartilage. Subsequent ossification is primarily dorsad and anterorad. By ca. 5 mm the anterior end of the articular extends anteriorly along the mesial surface of the dentary. A shallow notch, present on the posterodorsal margin of Meckel's cartilage, becomes the socket for the articular condyle of the quadrate. A posterior projection, which nearly reaches the anterior end of the preopercular, extends from the posterior margin of the articular, beginning at ca. 6 mm.

The angular ossifies from the posteroventral corner of Meckel's cartilage, beginning at ca. 4 mm, and articulates with the posteroventral margin of the articular.

HYOMANDIBULAR, SYMPLECTIC. An undivided hyomandibulosymplectic cartilage is present in the smallest cleared and stained specimen. Hyomandibular ossification begins in the vicinity of the facial nerve foramen before 4 mm, extends dorsally and laterally to the margins of the sphenotic and pterotic condyles by 4.3 mm, and spreads ventrad after ca. 4 mm. The opercular condyle remains cartilaginous until ca. 8.5 mm.

The symplectic is first visible (ca. 4 mm) as a thin ossifying sheath around the

lower part of the hyomandibulosymplectic cartilage. Except for extending farther along the length of the cartilage and becoming more heavily ossified, it does not change. The symplectic articulations with the quadrate and hyomandibular remain cartilaginous in the largest cleared and stained specimen.

ECTOPTERYGOID, MESOPTERYGOID, METAPTERYGOID, PALATINE, QUADRATE. The pterygoid bones, palatine, and quadrate all ossify from a single cartilage, which is absent in the smallest cleared and stained specimen, but is forming by ca. 3.5 mm. This cartilage initially appears as an inverted triangle with short dorsal anterior and posterior processes which subsequently (by ca. 4 mm) elongate (e.g., Fig. 6b). The mesopterygoid, followed quickly by the quadrate, are first to begin ossifying at about 4 mm (Table 2). The mesopterygoid ossifies from the dorsal margin along the middle of the cartilage, while the quadrate begins ossifying along its ventral condyle and subsequently fans out over most of the lower limb of the cartilage. The ectopterygoid begins ossifying along the lower margin of the anterior process of the cartilage at ca. 4.6 mm. The anterior margin of the developing quadrate reaches the posterior margin of the ectopterygoid at ca. 6.5 mm and overlaps it by ca. 20 mm. At this size (20 mm) the posterior dorsal margin of the quadrate articulates with the metapterygoid, and a posterior projection begins to extend from the lower posterior margin of the quadrate. This projection is just ventrad (and external) to the lower margin of the symplectic, and by ca. 23.5 mm it extends (dorsad) along most of the length of the lower limb of the preopercular.

The mesopterygoid becomes a large, elongate oval (in dorsal view), slightly cupped bone that extends from the lower margin of the eye to about one-quarter of the way up its mesial surface, by ca. 22.5 mm. The mesopterygoid articulates with the ectopterygoid at ca. 7 mm, and with the palatine and metapterygoid between ca. 20–23.5 mm. The anterodorsal margin of the metapterygoid slightly overlaps the posteroventral mesopterygoid margin by ca. 23.5 mm. The mesopterygoid and quadrate remain separated by a narrow band of cartilage in the largest cleared and stained specimen.

Metapterygoid ossification begins around the upper end of the posterior limb of the palato-pterygoquadrate cartilage at ca. 8.5 mm, and subsequently spreads down along the posterior limb to articulate with the quadrate and overlap the margin of the mesopterygoid. An interdigitating articulation between the upper end of the metapterygoid and the hyomandibular begins to form at ca. 23.5 mm. A posteriorly-projecting mesial metapterygoid flange (Johnson, 1980) does not develop by 23.6 mm (absent in all cleared and stained specimens).

The palatine is first visible at ca. 5.7 mm as a thin ossification along the anterior ventral margin of the palato-pterygoquadrate cartilage. The palatine subsequently ossifies around the cartilage, and extends posteriorly to articulate with the mesopterygoid and ectopterygoid by 12.4 mm. The palatine articulations with the lateral ethmoids and maxillaries remain cartilaginous in the largest cleared and stained specimen. There are no palatine teeth.

Opercular Series (Fig. 6, Table 2).—The preopercular and opercular are present in the smallest cleared and stained specimen (2.9 mm). At this size the preopercular has two spines on the posterior margin of the interior shelf, and one (much smaller) spine on the margin of the narrower exterior shelf. The full complement of 7–8 spines along the interior shelf is present by ca. 6 mm, and persists to at least 23.6 mm. The middle spine in this series typically is a bit longer than the others. The exterior shelf acquires a maximum of three small spines by ca. 4–4.5 mm; these become smaller and blunt during postflexion, then disappear between 9.3 and 12.2 mm. At the end of the larval stage the posterior margin of the exterior shelf

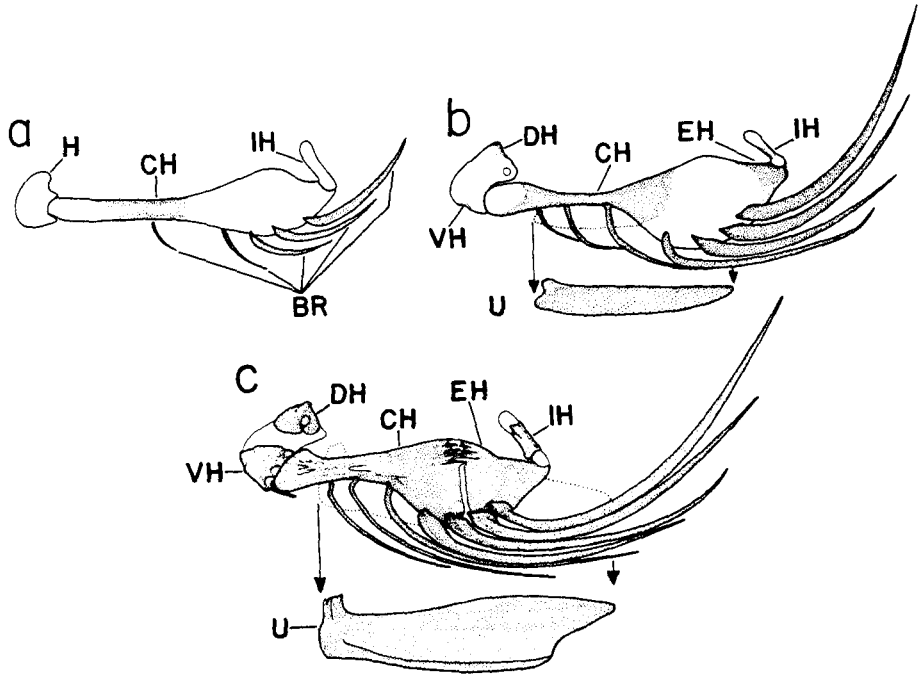

Figure 7. Development of the hyoid arch of sargo, *Anisotremus davidsonii*: a. 4.2 mm (SIO 91-135); b. 6.7 mm (SIO 91-135); c. 23.6 mm (SIO 62-346). White = cartilage; stippled = ossifying. Abbreviations are: BR = branchiostegals; CH = ceratohyal; DH = dorsal hypohyal; EH = epihyal; H = hypohyal cartilage; IH = interhyal; U = urohyal; VH = ventral hypohyal.

extends inward toward the interior shelf, and by ca. 20 mm it contacts the interior shelf midway along the length of the preopercular, forming part of the preoperculomandibular canal.

The opercular initially is a slender ossification extending from near the upper posterior margin of the hyomandibulosymplectic cartilage, along the upper posterior margin of the preopercular. It expands to a roughly triangular shape by ca. 4 mm, acquires a spine along the posterodorsal margin by ca. 8.5 mm, and may acquire a second, smaller spine near the top of the posterior margin by ca. 20 mm.

The subopercular and interopercular apparently begin forming simultaneously, at ca. 4 mm. The subopercular initially is a small, crescent-shaped dermal ossification just below the lower margin of the opercular. Subsequent changes consist largely of enlargement, and first acquiring, then losing, a spine along its lower margin (ca. 5–12 mm). The interopercular first appears as a slender blade-like dermal ossification with a single very small spine, just mesial to the middle of the posterior margin of the preopercular. It subsequently expands to become a broad, somewhat crescent-shaped bone, and acquires up to four more spines along its posterior margin by the end of the larval stage. The interopercular spines persist to at least 23.6 mm.

Hyoid Arch (Fig. 7, Table 2).—Development of the hyoid arch and branchiostegal rays in sargo is essentially identical to that described by Potthoff et al. (1984) for *Anisotremus virginicus*. Johnson (1980) noted that a ceratohyal beryciform fo-

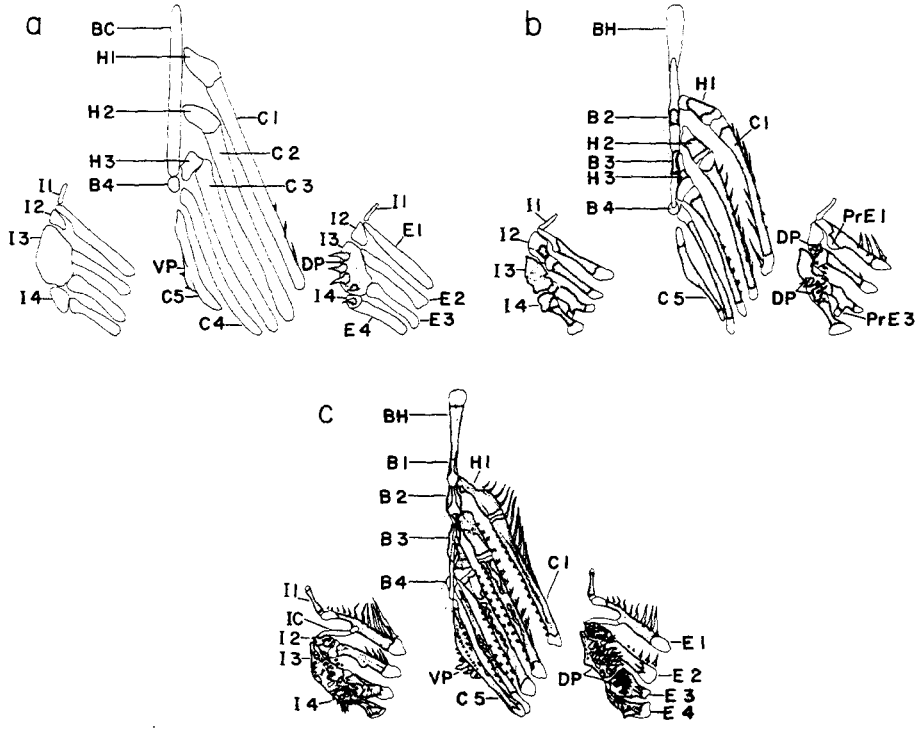

Figure 8. Development of the branchial arches of sargo, *Anisotremus davidsonii*: a. 4.2 mm (SIO 91-135); b. 6.7 mm (SIO 91-135); c. 23.6 mm (SIO 62-346). White = cartilage; stippled = ossifying. The left side of the branchial arches are shown in ventral view, with the epibranchials and dorsal tooth plates displaced laterally to the right in the figure. The right epibranchials and dorsal tooth plates are shown in dorsal view, displaced to the left in the figure. Abbreviations are: BC = basibranchial cartilage; B1–4 = basibranchials 1–4; C1–5 = ceratobranchials 1–5; DP = dorsal tooth plate; E1–4 = epibranchials 1–4; H1–3 = hypobranchials 1–3; IC = interarcual cartilage; I1–4 = pharyngobranchials 1–4; PrE1, 3 = process on epibranchials 1, 3; VP = ventral tooth plate.

ramen is present in the genus *Anisotremus*, and Potthoff et al. (1984, fig. 24) showed a feature that appeared to be this structure in juvenile *A. virginicus*; in sargo there is no evidence of the beryciform foramen in larvae or early juveniles (to 23.6 mm).

Branchial Arches (Fig. 8, Table 2).—Development of the branchial arches in sargo closely resembles that described for *A. virginicus* (Potthoff et al., 1984).

In sargo, basibranchials 2 and 3 may begin ossifying slightly before basibranchial 1 (e.g., Fig. 8b), in contrast to simultaneous ossification in *A. virginicus* (Potthoff et al., 1984). Tooth plates on epibranchials 2 and 3, present in a 21.5 mm specimen of *A. virginicus* (Potthoff et al., 1984), were not seen in sargo. The interarcual cartilage connecting epibranchial 1 with pharyngobranchial 2 apparently develops later (ca. 8.5 mm) in sargo than in *A. virginicus* (ca. 5.7 mm: Potthoff et al., 1984).

Axial Skeleton (Figs. 9, 10; Tables 2, 3).—VERTEBRAL COLUMN (Fig. 9). There are no neural or haemal arches or spines in the 2.9 mm larval sargo, but most are present as cartilage by ca. 4 mm. It could not be determined whether the arches develop from anterior, middle, and posterior sites along the notochord, as was

Table 3. Counts of fin spines and rays, vertebrae, ribs, gill rakers (outer arch: counts given as epibranchial, and hypobranchial + ceratobranchial; one raker at the ceratobranchial-epibranchial articulation is counted with the ceratobranchial rakers), and branchiostegal rays in *Anisotremus davidsonii*. Specimens between dashed lines are undergoing notochord flexion; those below the solid line are juveniles

Length (mm)	Fin rays						Vertebrae	Ribs		Gill rakers	Branchiostegal rays
	1°C	2°C	D	A	P_1	P_2		Pleural	Epipleural		
2.9											5
3.5											5
4.2	2+2									0+3	5
4.3	1+1									0+3	5
4.5	3+3						2			0+3	6
4.5	4+4									0+3	5
4.6	5+5						3			0+4	6
4.6	5+5						3			0+5	6
4.6	3+3										
4.7	5+5						3			0+5	6
4.7	8+8						10+3			0.6	6L,7R
5.0	5+5						6			0+4	6
5.2	8+8						10+5			0+5	7
5.4	8+8						10+3			0+5	7
5.4	8+8						10+3			0+7	7
5.4	9+8						10+4			0+6	7
5.4*	9+8		9	8			10+13			0+9L,8R	7
5.5	8+8						10+4			0+6	6
5.5	9+8		6	5			10+9			0+8	7
5.7	9+8						10+8			0+7	7L,6R
5.7	4+4									0+3	6
5.8	9+8	0+1	11	8			10+9			0+8	7

Table 3. Continued

Length (mm)	Fin rays						Vertebrae	Ribs		Gill rakers	Branchiostegal rays
	1°C	2°C	D	A	P_1	P_2		Pleural	Epipleural		
6.7	9+8	0+1	15	II,10	4		10+16			3+8	7
7.1	9+8	1+2	II,15	II,10	5		9+15			0+10	7
7.1	9+8	2+2	I+II,16	I,12	6		10+16			2+10	7
7.9	9+8	2+2	X,15	I,12	8	I,2	10+16			2+10	7
8.2	9+8	4+4	XI,14	III,10	11	I,3	10+16			2+10	7
8.2	9+8	4+4	X,15	II,11	11		10+16			—	7
8.4	9+8	3+3	X,14	II,11	10	I,1	10+16			3+12	7
8.8	9+8	2+3	II+II,13	I,12	7	I,1	10+16			3+13	7
12.1	9+8	9+8	XI,14	III,11	17	I,5	10+16	5	6	7+14	7
12.4	9+8	12+11	XI,15	III,10	17	I,5	10+16	8	6	7+13	7
12.9	9+8	10+9	XI,14	III,10	18	I,5	10+16	7	4	7+14	7
14.9	9+8	12+11	XI,15	III,10	18	I,5	10+16	8	6L, 7R	6+15	7
17.9	9+8	11+10	XI,14	III,9	18	I,5	10+16	8	8	7+16	7
19.9	9+8	12+11	XI,15	II,9	17	I,5	10+16	8	9	9+16	7
22.6	9+8	14+12	XI,15	III,10	18	I,5	10+16	8	9	9+15	7
23.6	9+8	13+13	XII,15	III,10	19	I,5	10+16	8	8	9L,11R+15	7

* Postflexion specimen, probably shrunken.

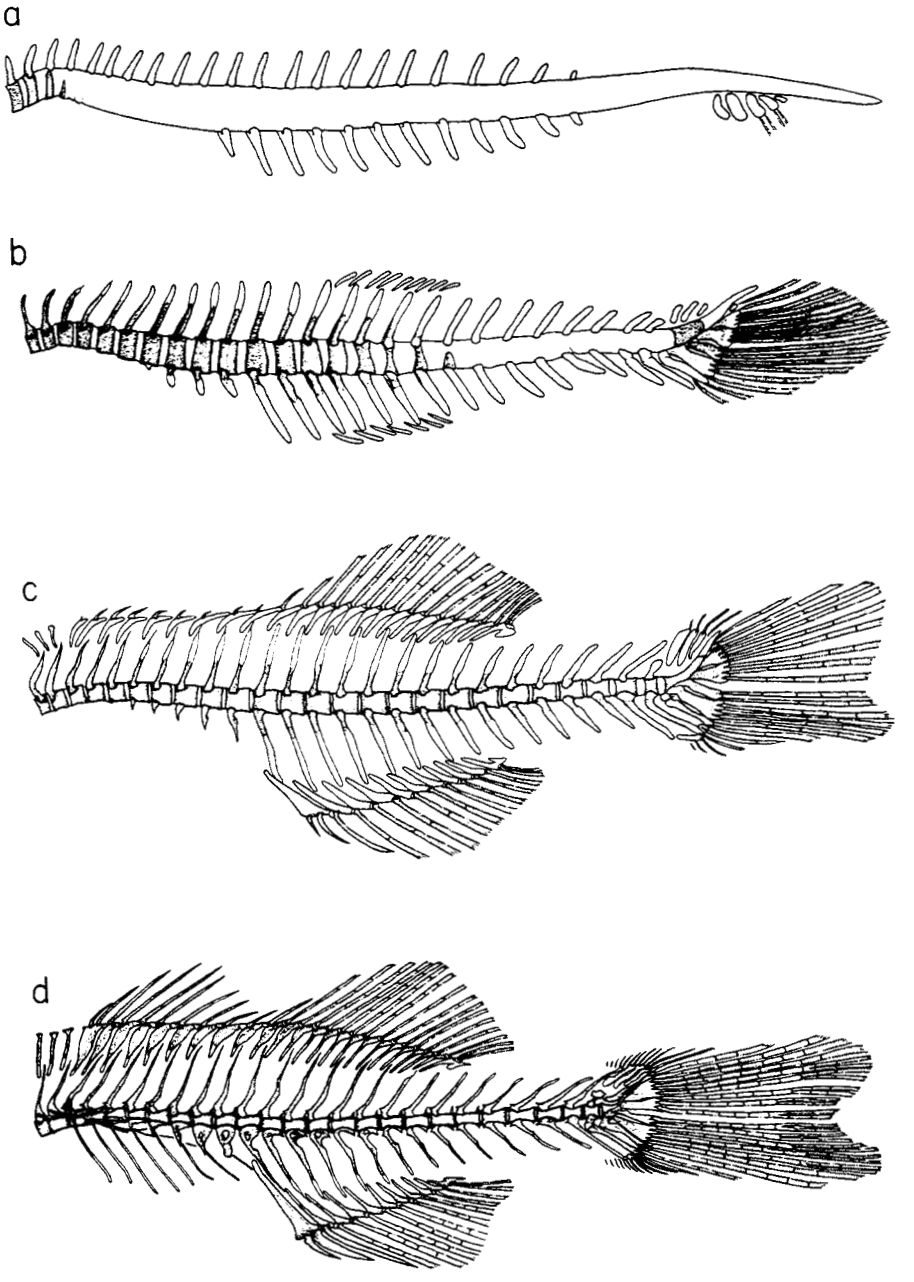

Figure 9. Development of the axial skeleton of sargo, *Anisotremus davidsonii*: a. 4.2 mm (SIO 91-135); b. 5.7 mm (SIO 91-135); c. 8.2 mm (SIO 91-135); d. 14.9 mm (SIO 91-136). White = cartilage; stippled = ossifying.

described for *A. virginicus* (Potthoff et al., 1984). Ossification of the arches and spines is anterior to posterior, and the arches on the abdominal vertebrae ossify distad from their bases in sargo as in *A. virginicus*. However, in contrast to *A. virginicus*, the arches on the caudal vertebrae in sargo apparently begin ossifying from just above their bases, and subsequently ossify both distad and proximad. Neural prezygapophyses develop on neural arches 3–25, and haemal prezygapophyses on haemal arches 11–25. These are first visible at 12.4 mm, on neural arches 3–23 and haemal arches 14–23.

Ossification of vertebrae begins at ca. 4.5 mm and is anterior to posterior, except that the urostyle ossifies before most caudal vertebrae. Each centrum begins ossifying as a thin ventral band between the proximal ends of its haemal arch. Ossification is dorsad from this ventral origin; when it has reached about one-third of the way up each side of the notochord, a dorsal saddle ossifies between the bases of the neural arch, then continues ventrad to meet the ascending arms of the ventral band. Neural postzygapophyses develop on centra 2–25, and haemal postzygapophyses develop on centra 10–23. These develop after 9.3 mm, and nearly all are present by 12.4 mm (neural postzygapophyses on centra 4–21 and haemal postzygapophyses on centra 10–21 in the 12.4 mm specimen). Neural and haemal postzygapophyses originate as small, laterally-paired, spine-like processes at the posterior dorsolateral and ventrolateral margins of each centrum, respectively. Low, thin, ossified flanges develop along each centrum, bridging from the "spines" to their adjacent (anterior) neural or haemal arches. These subsequently enlarge and acquire variable numbers and sizes of foramina.

Pleural and Epipleural Ribs. Eight pleural and eight or nine epipleural ribs develop in sargo. Larvae $\leq$9.3 mm have none, but in the 12.4 mm specimen centra 3–9 support seven pleural ribs and centra 1–4 support four epipleural ribs. The pleural ribs develop from cartilage; the epipleural ribs are dermal ossifications originating in the myosepta.

Caudal Fin (Fig. 10). The first visible caudal elements (ca. 4 mm) are the cartilaginous parhypural, cartilaginous hypurals 1–4, and four calcified fin rays supported by hypurals 2 and 3. In contrast to apparently simultaneous development in *A. virginicus*, the haemal spines of preural centra 2 and 3 develop after the parhypural and hypurals (except hypural 5) in sargo. Both are present as cartilage by 4.3 mm. Ossification of hypurals 1–3 begins at ca. 5.5 mm. The parhypural apparently begins ossifying at ca. 7 mm. Uroneurals develop later in sargo than in *A. virginicus*: sargo 12.1 mm or smaller have none (both pairs are present in all larger specimens), while both pairs are present by 6.2 mm in *A. virginicus* (Potthoff et al., 1984). Sargo apparently acquires only two ventral distal radial cartilages, in contrast to three for *A. virginicus* (Potthoff et al., 1984). None of the cleared and stained specimens had a separate radial cartilage adjacent to the tip of the haemal spine of preural centrum 2 (present in *A. virginicus*), and the other two radial cartilages do not shift in location as they do in *A. virginicus* (Potthoff et al., 1984). A radial cartilage is present at the distal tip of hypural 5 in *A. virginicus* (Potthoff et al., 1984); none was seen in sargo, although in the 23.6 mm juvenile the cartilaginous distal tip of hypural 5 appears to have been just beginning to separate into proximal and distal elements.

Dorsal and Anal Fins. The first elements to form in the dorsal and anal fins might be the cartilaginous pterygiophores of the middle soft rays: the 5.7 mm specimen has these pterygiophores and lacks dorsal and anal fin rays, but a 5.5 mm specimen and all specimens 5.8 mm and larger have both the pterygiophores and fin rays. In the 5.7 mm specimen (Fig. 9b), the dorsal and anal pterygiophores are those that would have supported dorsal rays 5–13 and anal rays 2–8. In the

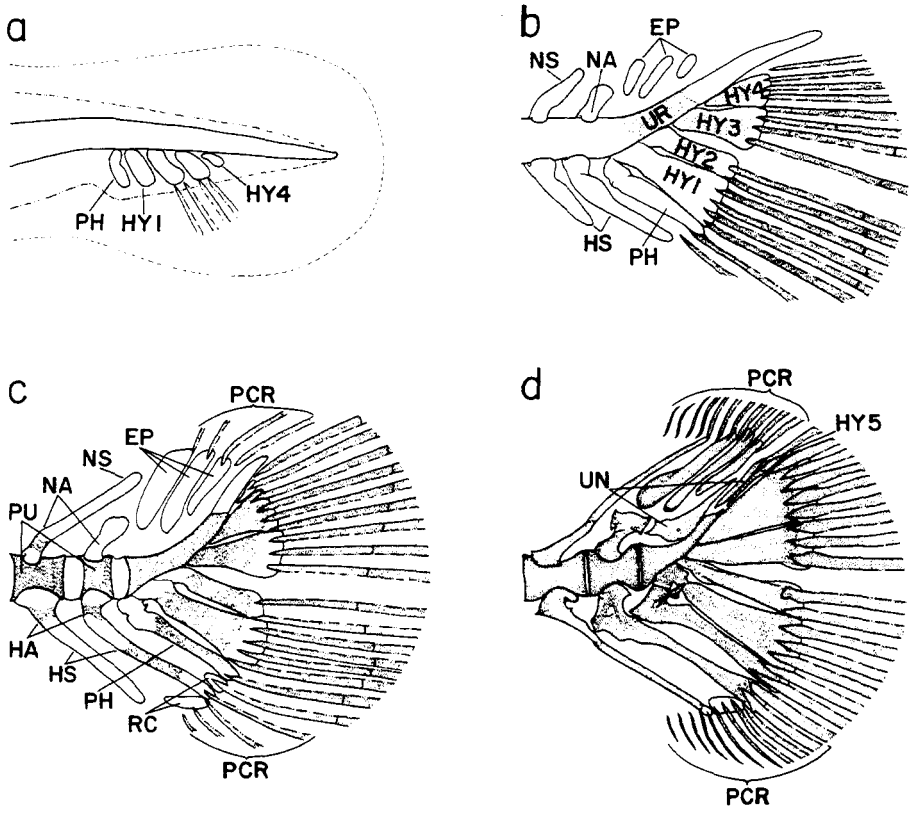

Figure 10. Development of the caudal skeleton of sargo, *Anisotremus davidsonii*: a. 4.2 mm (SIO 91-135); b. 5.5 mm (SIO 91-135); c. 8.2 mm (SIO 91-135); d. 14.9 mm (SIO 91-136). White = cartilage; stippled = ossifying. Abbreviations are: EP = epural; HA = haemal arch; HS = haemal spine; HY1–5 = hypurals 1–5; NA = neural arch; NS = neural spine; PCR = procurrent caudal ray; PH = parhypural; PU = preural centrum; RC = radial cartilage; UN = uroneural; UR = urostyle.

5.5 mm specimen, dorsal rays 5–10 and anal rays 2–6 are present already. Addition of pterygiophores is both anterior and posterior in the anal and second dorsal fins, and may be posterior to anterior in the first dorsal: only the posterior three dorsal spine pterygiophores are present at 6.6 mm, and all are present in specimens 6.7 mm and larger. Addition of soft rays is both anterior and posterior in both fins. Addition of dorsal spines begins anteriad from the posteriormost spine; spines II–III or IV appear about simultaneously with spine IX or X, and then the middle spines probably are added from anterior to posterior. The first spine is added about simultaneously with spine IV or V. Development of the individual dorsal and anal pterygiophores, spines, and rays is the same as was described for *A. virginicus*, except that it is unclear whether both the second and third anal spines, or only the third, develop from rays in *A. davidsonii* (both the second and third spines develop from rays in *A. virginicus*: Potthoff et al., 1984). The first dorsal pterygiophore, which supports the first two spines, originates as two separate cartilages in sargo as in *A. virginicus*: these separate cartilages were seen in the 8.2 mm specimen (Fig. 9c). It could not be determined whether the first anal pterygiophore originates as one or two cartilages in sargo (there are two in *A.*

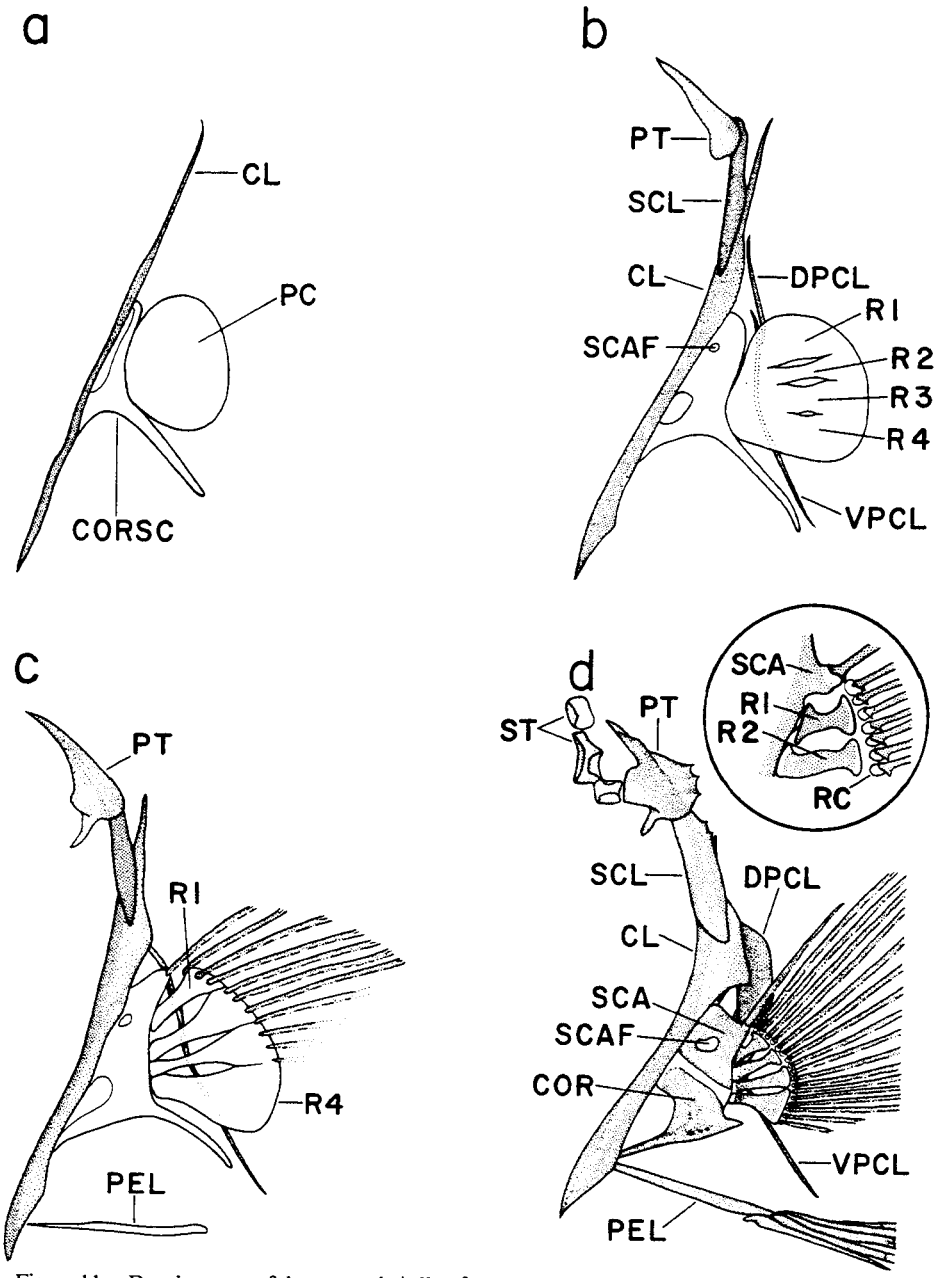

Figure 11. Development of the pectoral girdle of sargo, *Anisotremus davidsonii*: a. 2.9 mm (SIO 91-135); b. 6.7 mm (SIO 91-135); c. 8.2 mm (SIO 91-135); d. 14.9 mm (SIO 91-136). White = cartilage; stippled = ossifying. Abbreviations are: CL = cleithrum; COR = coracoid; CORSC = coracoscapular cartilage; DPCL = dorsal postcleithrum; PC = cartilaginous pectoral blade; PEL = pelvis; PT = post-temporal; RC = cartilaginous distal radial; R1–4 = proximal radials 1–4; SCA = scapula; SCAF = scapular foramen; SCL = supracleithrum; ST = supratemporal; VPCL = ventral postcleithrum.

virginicus). Separate cartilages were not seen in any specimen, but the 8.4 mm specimen had a large foramen (absent in all others) near the anterior distal margin of the pterygiophore, that nearly separated a thin, crescent-shaped anterior section from the remainder of the pterygiophore. This anterior section might have originated as a separate cartilage that was in the process of fusing with the principal part of the pterygiophore in the 8.4 mm specimen.

Pectoral and Pelvic Girdle (Fig. 11, Table 2).—Development of the pectoral and pelvic fins and their supporting bones is essentially the same in sargo as was described for *A. virginicus* (Potthoff et al., 1984). Initial development of the pectoral proximal radials could not be tracked in sargo. The 2.9 mm specimen has an undivided pectoral cartilage (Fig. 11a), while the 6.7 mm specimen has all three cleavages that define the four radials (Fig. 11b). The pectoral blade or radial cartilages did not stain with alcian blue in any of the intermediate-size specimens. Ossification of the proximal radials apparently begins later in sargo than in *A. virginicus*: none were ossifying through 9.3 mm, but radials 1–3 were ossifying in the 12.4 mm specimen, and all four were ossifying by 14.4 mm, in contrast to ossification beginning between 8.6–10.4 mm in *A. virginicus*. The cartilaginous distal pectoral radials were first seen at 14.4 mm. Supratemporal bones were not visible in specimens 9.3 mm or smaller, but were well developed in all specimens 12.4 mm and larger.

Xenistius californiensis

Pigmentation (Figs. 12–15).—Salema is lightly pigmented throughout most of the larval stage, closely resembling sargo during the preflexion stage. During preflexion 14 to 22 melanophores (mode = 16), usually of similar size and beginning at the first or second postanal myomere, are spaced uniformly (ca. 1 per myomere) along the ventral margin of the tail. Unlike preflexion-stage sargo, larval salema lack the melanophore embedded above the hindgut at the last preanal myomere, but as in sargo the number of melanophores along the ventral margin of the tail decreases to 10–19 (mode = 15) during notochord flexion and to 11–16 (mode = 13) in the postflexion stage. After the anal fin anlage begins to develop (ca. 4.3 mm), the first one or two melanophores (anterior to the anal fin base) usually move internally and disappear, and the next five to nine move ventrad onto the sides of the developing anal fin ray bases. The last melanophore along the anal fin base usually is embedded above the last ray base. During the early juvenile stage the melanophores along the peduncle move internally. At the end of the larval stage small melanophores develop along the anal fin rays (beginning as early as 15.5 mm). The amount of pigmentation is variable, from nearly absent to moderately heavy; when present, pigment is heaviest anteriorly between the first spine and fourth ray.

During the preflexion stage, 0–3 (mode = 1) small melanophores occur under the notochord tip; these become situated at the base(s) of any one (or more) of the four lowermost principal caudal rays (rarely, pigment is present at an upper caudal ray base, as well). At the end of the larval stage (ca. 15.5 mm) and during the early juvenile stage small melanophores develop along the sides of most principal caudal fin rays. This pigmentation tends to be densest along the middle rays, but a clear pattern (as in sargo) is absent.

Little or no pigment develops on the dorsal or lateral surfaces of the trunk and tail until the end of larval development (Fig. 14). The smallest specimen with dorsal trunk and tail pigment (15.5 mm) had this pigment in four areas: just anterior to the first dorsal spine (two pairs of melanophores), along each side of

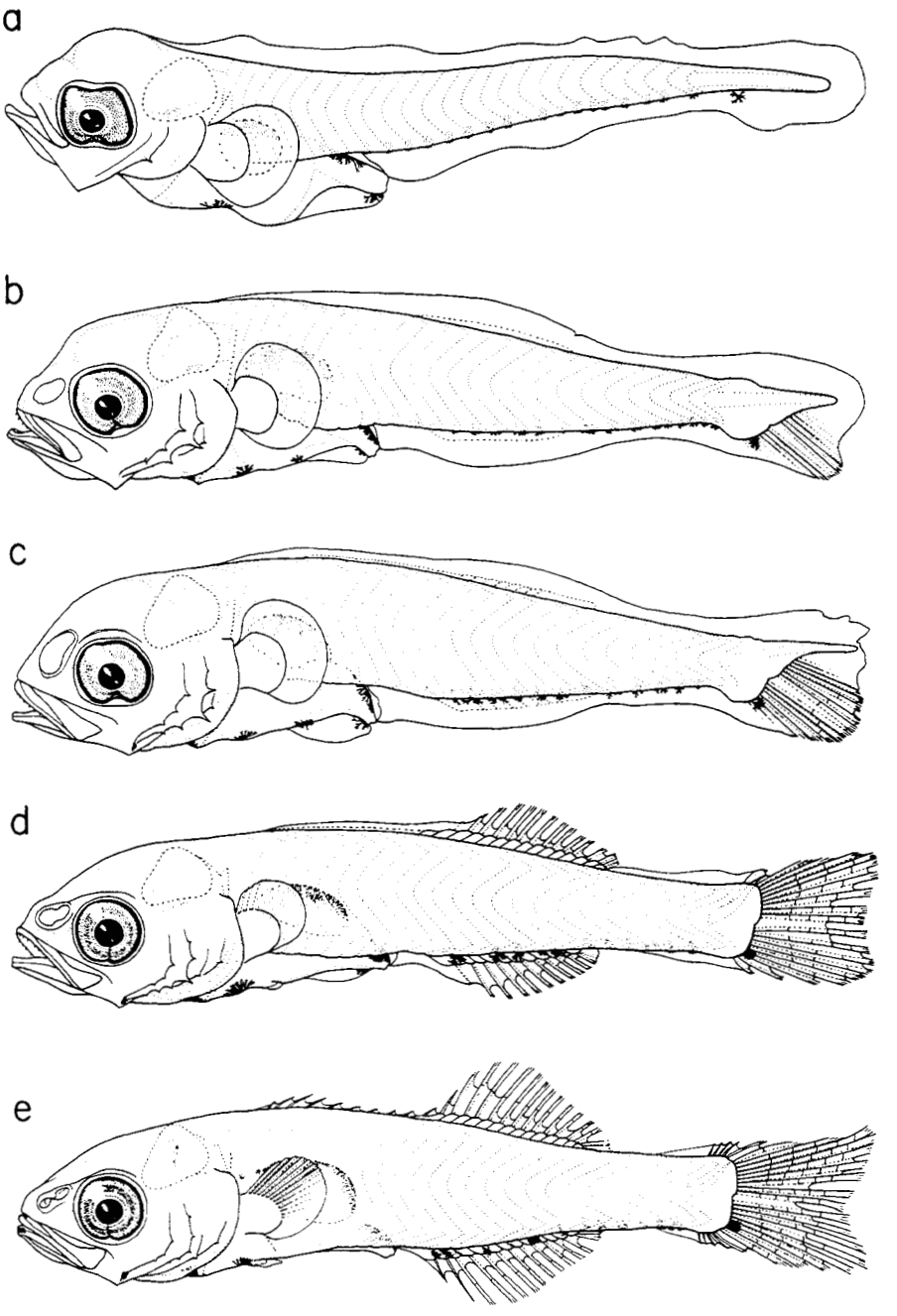

Figure 12. Larval salema, *Xenistius californiensis* (all SIO 91-135): a. 3.2 mm; b. 5.1 mm; c. 5.9 mm; d. 7.8 mm; e. 9.5 mm.

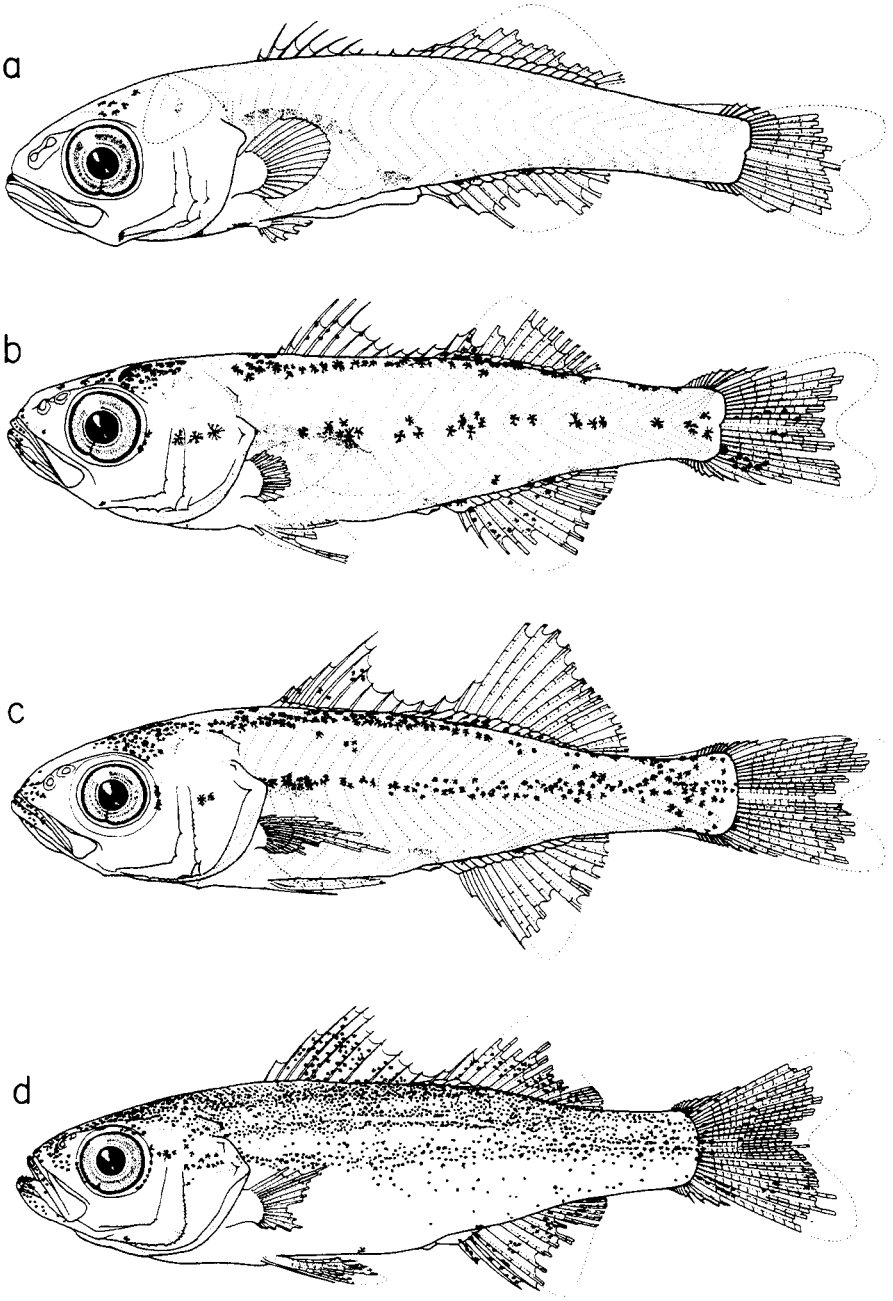

Figure 13. Larval (a), transforming (b, c), and juvenile (d) salema, *Xenistius californiensis*: a. 12.9 mm (SIO 91-135); b. 15.5 mm (SIO 62-356); c. 20.6 mm (SIO 62-742); d. 32.2 mm (SIO 62-356).

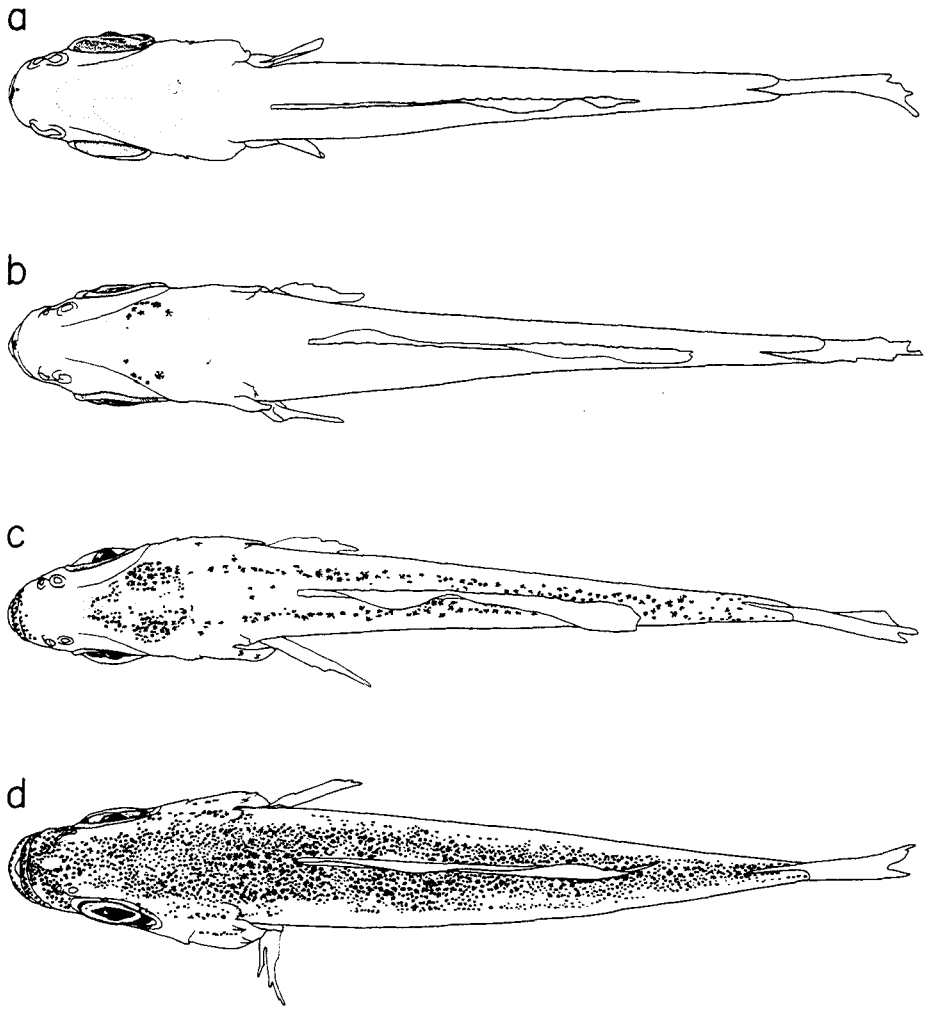

Figure 14. Larval (a, b), transforming (c), and juvenile (d) salema, *Xenistius californiensis*, in dorsal view: a. 9.5 mm (SIO 91-135); b. 12.9 mm (SIO 91-135); c. 20.6 mm (SIO 62-742); d. 32.2 mm (SIO 62-356).

the dorsal fin base from the fifth spine to the last ray (this pigment is continuous anteriorly with the dorsolateral diagonal band), midway along the caudal peduncle (five melanophores) and just anterior to the dorsal procurrent caudal fin rays (one melanophore). During the early juvenile stage dorsal melanophores fill in between these areas and scattered dorsolateral melanophores develop on the peduncle and below the dorsal fin (ca. 21 mm). Melanophores essentially cover the upper half of the body by ca. 32 mm; three longitudinal stripes (two are dorsolateral) are discernable at this size (Fig. 13d).

A few scattered melanophores develop on the membranes between the anterior six dorsal spines and anterior two rays at ca. 15.5 mm. Dorsal fin pigmentation is variable, but in juveniles larger than 21.8 mm it typically is heavy on the

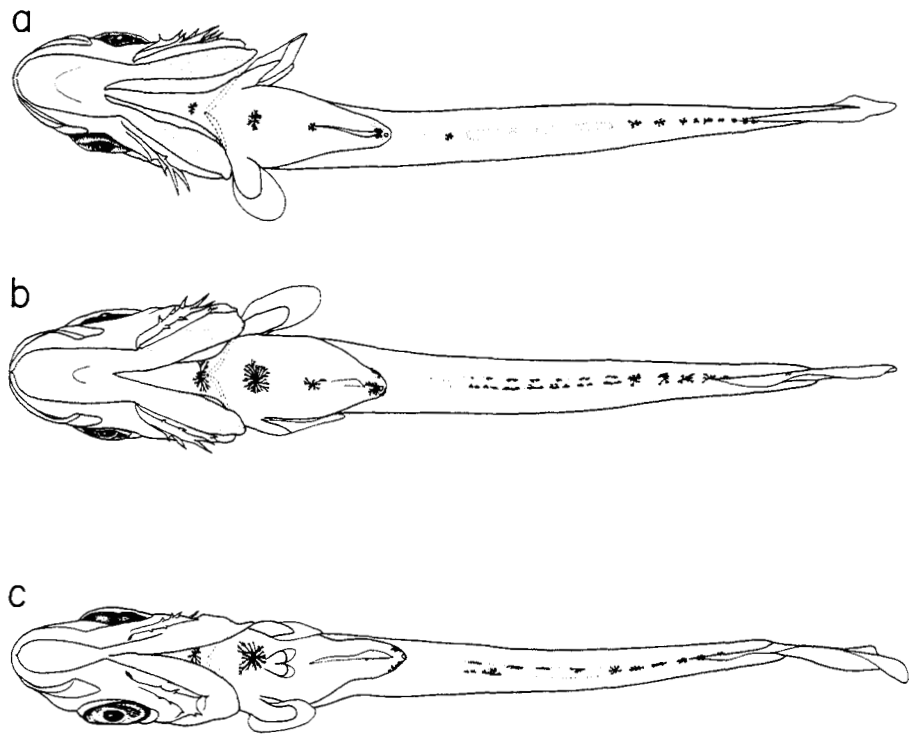

Figure 15. Larval salema, *Xenistius californiensis*, in ventral view (all SIO 91-135): a. 5.1 mm; b. 5.9 mm; c. 7.8 mm.

membranes between all the spines and along the outer half of the membranes between all rays.

Lateral trunk and tail pigment develops simultaneously with the dorsal trunk and tail pigment. The smallest specimen with lateral midline pigment (15.5 mm) had this pigment arranged in six patches (two to six melanophores in each patch) between the level of the swimbladder and the end of the peduncle. Melanophores quickly fill in between these patches (by ca. 20.6 mm) and the resulting band broadens, beginning posteriorly and progressing anteriorly. The dorsolateral and lateral pigment meet at the level of the soft dorsal fin by ca. 32 mm; at this size a few scattered (mostly myoseptal) ventrolateral melanophores are present.

The gut is always pigmented dorsally (internally) and ventrally (externally). However, anterior pigment, such as is seen in sargo, does not develop and external lateral pigment on the gut area is absent or nearly so until the end of the larval stage.

During the preflexion stage dorsal gut pigment (including swimbladder pigment) consists of one to three large melanophores covering the dorsal surface of the swimbladder (present in 97% of the specimens) and one (in 97%) or two (3%) large melanophores on the dorsal surface of the posterior hindgut. During the flexion stages the swimbladder pigment (always present) expands to cover its dorsal, dorsolateral and posterior surfaces. Swimbladder and hindgut pigment subsequently change little; an unpigmented area over the anterior hindgut nearly

always separates these (unpigmented area absent in only one of the 124 larvae examined). In about 5% of postflexion-stage specimens dorsal pigment develops on the gut, just anterior to the swimbladder.

Ventral pigment on the gut consists of one to six external melanophores along the ventral midline from the anterior midgut to the posterior hindgut. The number of melanophores decreases during larval development (Fig. 15), from a modal number of 3 (range 1–6) during the preflexion stage to 1 (range 0–4) during the postflexion stage, then to zero in juveniles (none visible by 21.8 mm). The first melanophore in this series is located at the pelvic fin base. The smaller melanophores along the posterior midgut and on the posterior hindgut typically persist only through the preflexion stage.

Lateral pigment on the abdominal area is absent through ca. 13 mm, remains sparse or absent until the lateral midline stripe develops, and typically is light up to the largest specimen examined (41.7 mm).

Head pigmentation during the preflexion stage usually is restricted to a melanophore on the ventral surface of the hindbrain (present in 90% of preflexion and all later specimens examined) and one on the isthmus just anterior to the cleithral symphysis (present in 68% of preflexion, and all later specimens). Near the end of notochord flexion (ca. 5.9 mm) a melanophore develops on each side of the posterior lateral surface of the midbrain (present in 11% of flexion and 89% of postflexion-stage specimens). An additional one or two posterior lateral midbrain melanophores may develop during the postflexion stage, although more commonly proliferation of this pigment does not begin until the end of larval development.

A few external dorsolateral melanophores develop on each side of the midbrain region beginning late in the postflexion stage (Fig. 14b). This pigment rapidly proliferates early in the juvenile stage to cover most of the dorsal and dorsolateral fore- and midbrain regions by ca. 21 mm (Fig. 14c), merging with the dorsal and dorsolateral trunk pigment by ca. 28 mm.

Melanophores first appear on the jaws during the postflexion stage (present in 10% of postflexion specimens smaller than 8 mm, and in 50% of those 8 mm or larger). During the larval stage this pigment consists of one or two melanophores at the premaxillary symphysis, occasionally with corresponding melanophores on the dentary (dentary pigment present in 25% of those larvae having upper jaw pigment). Pigment always is present across the anterior margins of both jaws during the juvenile stage, spreading upward across the snout and merging with the pigment over the brain by ca. 32 mm (Fig. 14d). The lower jaw pigment usually spreads downward and posteriorly onto the anterior gular membrane at the same time (gular pigment present in 5 of 7 juvenile specimens).

The only other head pigment during the larval stage is a melanophore at each angular. This may develop during the preflexion stage, as early as 3.8 mm, but more commonly is absent until ca. 5.1 mm (present in 12% of larvae 3.8–5.0 mm and in 90% of those larger than 5 mm).

During transformation to the juvenile stage (ca. 15.5 mm) pigment develops along the upper operculum, becoming continuous with the lateral midline stripe between ca. 21 and 28 mm. No other pigment develops on the head through the largest size examined (41.7 mm).

Morphology.—The smallest salema examined (2.2 mm) had no yolk or oil droplet. At this size the eye is pigmented, the mouth is functional, the swimbladder is inflated, and the gut is tubular and folded into a broad "S" shape. This fold tightens, forming a coil in the midgut between 3.8 and 4.0 mm. Notochord flexion begins at 4.3 mm and is completed between 5.9 and 6.2 mm. Transformation to

Table 4. Summary of measurements (in mm) of *Xenistius californiensis*. Body lengths are notochord length for preflexion and flexion-stage larvae, and standard length for postflexion and juvenile specimens. Measurements of body parts are summarized over 1 mm size classes; for each summary the mean measurement ($\bar{x}$), standard deviation (SD) and number of specimens measured (N) is given. Most specimens undergoing notochord flexion fall between the dashed lines below (the actual range of specimens undergoing notochord flexion is 4.3–6.2 mm); specimens below the dotted line are juveniles

Body length	Snout length			Eye diameter			Head length			Pre-Anus length			Pre-Dorsal fin length			Pre-Anal fin length			Body depth			Longest pre-opercular spine		
(mm)	$\bar{x}$	SD	N	$\bar{x}$	SD	N	$\bar{x}$	SD	N	$\bar{x}$	SD	N	$\bar{x}$	SD	N	$\bar{x}$	SD	N	$\bar{x}$	SD	N	$\bar{x}$	SD	N
2.0–2.9	0.1	0.03	8	0.3	0.02	9	0.6	0.1	9	1.1	0.1	9							0.5	0.1	9	0.02	0.02	9
3.0–3.9	0.2	0.04	17	0.3	0.03	17	0.9	0.1	17	1.5	0.2	17							0.7	0.1	17	0.1	0.03	17
4.0–4.9	0.3	0.1	13	0.4	0.03	13	1.2	0.1	13	2.0	0.2	13	2.1	0.3	2	2.5	0.4	5	1.0	0.1	13	0.1	0.02	13
5.0–5.9	0.5	0.1	13	0.5	0.1	13	1.6	0.2	13	2.6	0.2	13	2.3	0.4	13	3.0	0.2	13	1.2	0.1	13	0.1	0.02	13
6.0–6.9	0.6	0.03	17	0.6	0.04	17	2.0	0.1	17	3.3	0.2	17	2.5	0.5	15	3.6	0.2	17	1.5	0.1	17	0.1	0.03	17
7.0–7.9	0.6	0.1	28	0.7	0.1	27	2.2	0.2	28	3.8	0.2	28	3.0	0.7	28	4.1	0.2	28	1.6	0.1	28	0.1	0.02	28
8.0–8.9	0.8	0.1	16	0.8	0.1	16	2.6	0.1	16	4.4	0.2	16	3.1	0.4	15	4.7	0.2	16	1.8	0.1	16	0.1	0.02	16
9.0–9.9	0.8	0.04	8	0.9	0.1	8	2.9	0.2	8	4.9	0.2	8	3.2	0.1	8	5.1	0.2	8	2.0	0.1	8	0.1	0.02	8
10.0–10.9	0.8	0.03	2	0.9	0.1	2	2.9	0.3	2	4.9	0.6	2	3.2	0.3	2	5.1	0.6	2	2.0	0.2	2	0.1	0	2
13.0–13.9	1.2	—	1	1.4	—	1	4.5	—	1	7.9	—	1	5.4	—	1	8.1	—	1	3.1	—	1	0.1	—	1
15.0–15.9	1.4	—	1	1.6	—	1	5.4	—	1	9.2	—	1	5.8	—	1	9.4	—	1	3.8	—	1	0.1	—	1
21.0–21.9	1.9	0.3	2	2.1	0.1	2	7.4	0.6	2	13.1	0.1	2	7.8	0.2	2	13.1	0.1	2	5.8	0.1	2	0.1	0.04	2
28.0–28.9	2.4	—	1	2.8	—	1	9.6	—	1	12.5	—	1	10.7	—	1	12.5	—	1	7.8	—	1	0.1	—	1
29.0–29.9	2.3	—	1	2.9	—	1	9.8	—	1	17.2	—	1	10.3	—	1	17.2	—	1	7.8	—	1	0.1	—	1
30.0–30.9	2.3	—	1	3.1	—	1	10.2	—	1	18.2	—	1	10.8	—	1	18.2	—	1	8.5	—	1	0.1	—	1
32.0–32.9	2.8	—	1	3.0	—	1	10.8	—	1	19.4	—	1	11.1	—	1	19.4	—	1	8.8	—	1	0.1	—	1

the juvenile stage (indicated by scale formation, which is anterior to posterior) begins at ca. 15.5 mm and is complete by ca. 21 mm.

Larval development is a gradual process with no marked changes in body proportions (Figs. 12, 13; Table 4). Snout length, head length and pre-anus length all increase slightly relative to standard length during larval life. Snout length increases from an average 6% of standard length (range 3–7%) during the preflexion stage to 8% (range 6–10%) during notochord flexion and 9% (range 6–12%) in the postflexion and juvenile stages. Mean proportions (and ranges) for head length are: preflexion stage 25% (22–28%), flexion stage 29% (26–32%), postflexion stage 30% (27–35%), and juvenile 34% (33–36%). Respective values for pre-anus length are 44% (37–47%), 47% (44–53%), 52% (48–56%), and 57% (43–61%). Pre-dorsal fin length decreases as the fin develops, from a mean of 42% of standard length (range 32–53%) during notochord flexion to 39% (28–60%) in the postflexion stage and 36% (34–37%) in juveniles. Pre-anal fin length remains 55% (49–66%) of standard length throughout larval development. Similarly, body depth and eye diameter change little relative to standard length: depth averages 22% (15–26%) throughout larval life (but increases to 27%—range 26–28%—during the early juvenile stage), while eye diameter averages 10% (8–11%) through larval and early juvenile development.

Skeletal Development.—Alizarin staining of larval salema was less successful than the staining of sargo, and as a result, the sequence of developmental events was less fully determined. Nevertheless, from the material available, it appears that skeletal development differs little between the two species. Consequently, the description of skeletal development of salema is largely limited to Figures 16–22 and Tables 5–6; the narrative description consists of listings of differences from sargo, and limited supplemental information.

Neurocranium (Fig. 16, Table 5).—CHONDROCRANIUM. Development of the nasal septum is slightly later in sargo than in salema (ca. 4.2 mm vs. ca. 3.9 mm, respectively). The epiphysial cartilage is narrower and the anterior projection of the synotic tectum (prior to formation of the longitudinal cartilage between the synotic tectum and epiphysial cartilage) is smaller in salema than in sargo.

FRONTAL, PARIETAL. The parietal is somewhat narrower in salema than in sargo (Figs. 5, 16).

BASIOCCIPITAL, EXOCCIPITAL, SUPRAOCCIPITAL. The supraoccipital crest is smaller than that in sargo, and it does not acquire serrations along its dorsal margin (Figs. 5d, 16e).

BASISPHENOTIC, PARASPHENOTIC, PTEROSPHENOTIC, SPHENOTIC. There are no notable differences.

VOMER. The vomer begins to ossify at a slightly smaller size in salema (ca. 4.9 mm) than in sargo (ca. 6.5 mm), and apparently always lacks teeth. The vomer initially consists of two separate, slender ossifications: one forms on each side of the anterior margin of the ethmoid plate. These join mesially (5.5 mm) to form a slender crescent, just as in sargo.

EPIOTIC, PROOTIC, PTEROTIC. There are no notable differences.

LATERAL ETHMOID, MEDIAN ETHMOID. There are no notable differences.

NASAL. The nasals may begin to ossify slightly later in salema than in sargo (ca. 9.5 mm vs. ca. 8.5 mm, respectively).

CIRCUMORBITALS. The sequence of circumorbital ossification in salema could not be determined, except that the lacrymal is first, as in sargo. Development of the lacrymal begins earlier in salema than in sargo (ca. 5 mm vs. ca. 7 mm, respectively).

Table 5. Summary of skeletal development of *Xenistius californiensis*: size (mm SL) of smallest cleared and stained specimen with given structure visible as cartilage, or beginning to ossify; D = dermal origin

Structure	Size at first appearance of	
	Cartilage	Ossification
Neurocranium		
Basioccipital		3.9
Exoccipital		3.9
Parasphenotic		3.9
Pterosphenotic		7.4
Basisphenotic		21.2
Vomer		4.9
Lateral ethmoid		4.9
Median ethmoid		21.2
Lachrymal	D	4.9
Circumorbital 2	D	21.2
3	D	21.2
4	D	21.2
5	D	21.2
Dermosphenotic	D	21.2
Frontal	D	5.5
Parietal	D	6.8
Supraoccipital	D	4.9
Sphenotic		6.0
Pterotic		4.9
Prootic		4.9
Epiotic		6.0
Nasal	D	9.6
Jaws and suspensorium		
Premaxillary		3.9
Maxillary		2.7
Dentary	2.7	3.9
Articular	2.7	4.1
Angular	2.7	4.1
Hyomandibular	2.7	4.1
Symplectic	2.7	4.1
Quadrate	4.1	4.9
Ectopterygoid	4.1	5.9
Mesopterygoid		4.1
Metapterygoid	4.9	6.0
Palatine	5.8	6.0
Opercular series		
Preopercular	D	4.1
Opercular	D	4.1
Subopercular	D	4.9
Interopercular	D	4.9
Hyoid arch		
Branchiostegal	D	3.9
Ceratohyal	2.7	4.4
Epihyal	2.7	4.4
Interhyal	2.7	4.4
Ventral hypohyal	2.7	4.9
Dorsal hypohyal	2.7	6.0
Urohyal	D	4.9
Basihyal	4.9	7.4
Branchial arch		
Ceratobranchial	2.7	4.9
Epibranchial	4.4	4.9

Table 5. Continued

Structure	Size at first appearance of	
	Cartilage	Ossification
Hypobranchial	4.4	6.0
Basibranchial	4.4	6.0
Pharyngobranchial	4.4	7.4
Axial skeleton		
Vertebral centra		4.4
Urostyle		5.5
Neural arches	4.4	4.9
Haemal arches	4.4	5.9
Neural spines	4.4	9.6
Haemal spines	4.4	21.2
Epipleural ribs	D	9.6
Pleural ribs		9.6
Epurals	4.9	21.2
Hypurals 1–4	4.4	5.5
Hypural 5	6.3	9.6
Parhypural	4.4	5.5
Uroneurals	D	9.6
Caudal distal radials	9.6	
Dorsal pterygiophores	4.9	
Proximal radials	7.4	9.6
Distal radials	7.4	9.6
Anal pterygiophores	4.9	
Proximal radials	7.4	9.6
Distal radials	7.4	9.6
Pectoral and pelvic girdle		
Cleithrum		2.7
Supracleithrum	D	4.4
Dorsal postcleithrum	D	7.4
Ventral postcleithrum	D	4.9
Posttemporal	D	4.9
Supratemporals	D	21.2
Scapula	2.7	6.0
Coracoid	2.7	6.0
Pectoral proximal radials	4.9	21.2
Pectoral distal radials	21.2	
Basipterygia	7.4	21.2

Jaws and Suspensorium (Fig. 17, Table 5).—MAXILLARY, PREMAXILLARY, ROSTRAL CARTILAGE. The smallest cleared and stained specimen (2.7 mm) has a pair of long, slender, ossifying maxillaries, but apparently lacks premaxillaries. Small triangular premaxillaries are first visible at ca. 4 mm, and the rostral cartilage first appears at 4.5 mm.

ANGULAR, ARTICULAR, DENTARY. The lower jaw of the smallest cleared and stained specimen (2.7 mm) consists only of the slender Meckel's cartilages. Dentary ossification is first evident along the anterodorsal margin of each cartilage at ca. 4 mm. Dentary teeth apparently do not develop until ca. 4.5 mm, and form initially along the posterior half of each dentary instead of anteriorly, as in sargo.

HYOMANDIBULAR, SYMPLECTIC. There are no notable differences.

ECTOPTERYGOID, MESOPTERYGOID, METAPTERYGOID, PALATINE, QUADRATE. Ossification of the palato-pterygoquadrate cartilage may begin later in salema than in sargo (Tables 2, 5).

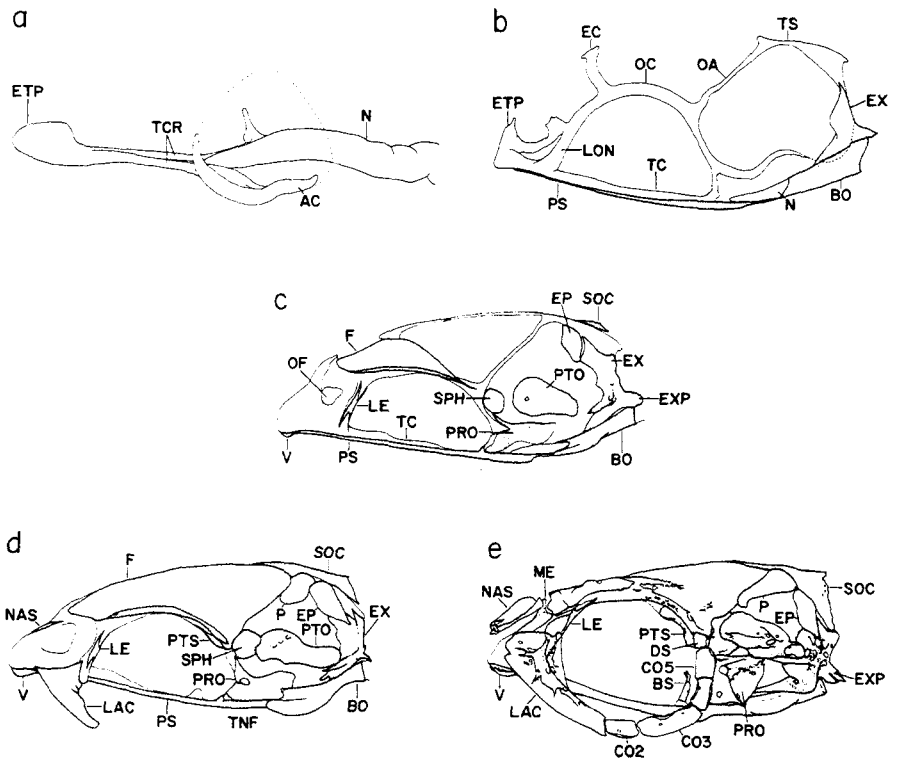

Figure 16. Lateral view of the developing neurocranium of salema, *Xenistius californiensis*: a. 2.7 mm (SIO 91-135); b. 4.1 mm (SIO 91-135); c. 7.4 mm (SIO 91-135); d. 9.6 mm (SIO 91-135); e. 21.2 mm (SIO 62-356). White = cartilage; stippled = ossifying. Abbreviations are: AC = auditory capsule; TCR = trabecula cranii. All other abbreviations are defined in Figure 5.

Opercular Series (Fig. 17, Table 5).—Although the preoperculum and operculum were not visible until 4.1 mm in the cleared and stained salema (Table 5), the first preopercular spine was clearly visible in an unstained 3.2 mm specimen (Fig. 12a), indicating that development begins at about the same size as in sargo (ca. 2.9 mm). The numbers of spines along the margins of the interior and exterior preopercular shelves differ little between the two species through at least 9.8 mm, but by ca. 21 mm salema has about twice as many small spines along the margin of the interior (posterior) shelf (Figs. 6d, 17d). The uppermost opercular spine of salema is distinctly larger than that of sargo (Figs. 6d, 17d).

The subopercular and interopercular were first visible at 4.9 mm, vs. 4.2 mm in sargo. Larval salema develop only a single interopercular spine, compared with four or five in sargo.

Hyoid Arch (Fig. 18; Tables 5, 6).—Development of the bones of the hyoid arch apparently is slightly precocious in salema, relative to development in sargo (Tables 2, 5).

Branchial Arches (Fig. 19; Tables 5, 6).—In contrast to the hyoid arch, development of the bones of the branchial arches may be slightly delayed in salema, relative to development in sargo (Tables 2, 5). There are slight differences in the

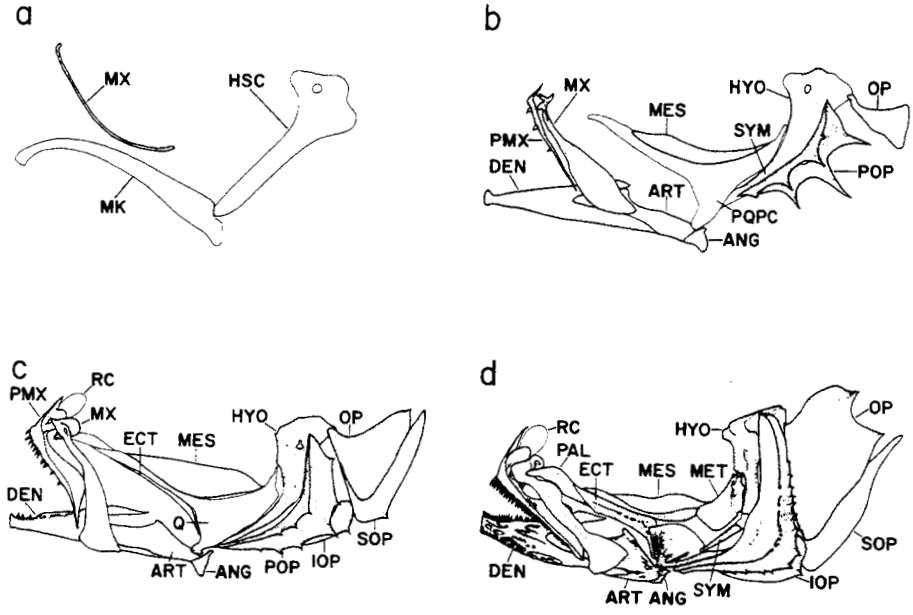

Figure 17. Development of the jaws, suspensorium, and opercular bones of salema, *Xenistius californiensis*: a. 2.7 mm (SIO 91-135); b. 4.1 mm (SIO 91-135); c. 9.6 mm (SIO 91-135); d. 21.2 mm (SIO 62-356). White = cartilage; stippled = ossifying. Abbreviations are defined in Figure 6.

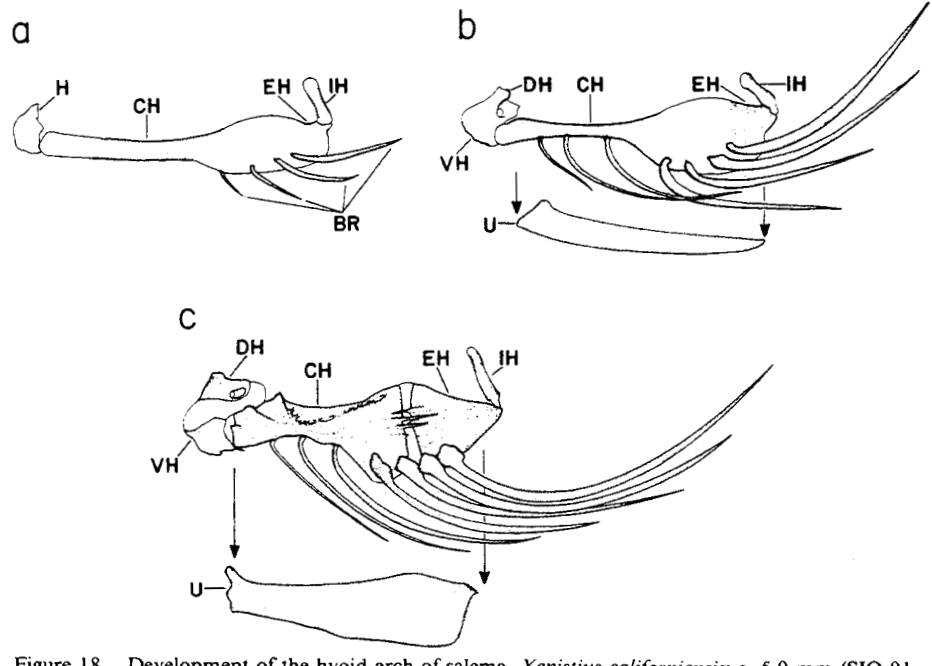

Figure 18. Development of the hyoid arch of salema, *Xenistius californiensis*: a. 5.9 mm (SIO 91-135); b. 7.4 mm (SIO 91-135); c. 21.2 mm (SIO 62-356). White = cartilage; stippled = ossifying. Abbreviations are defined in Figure 7.

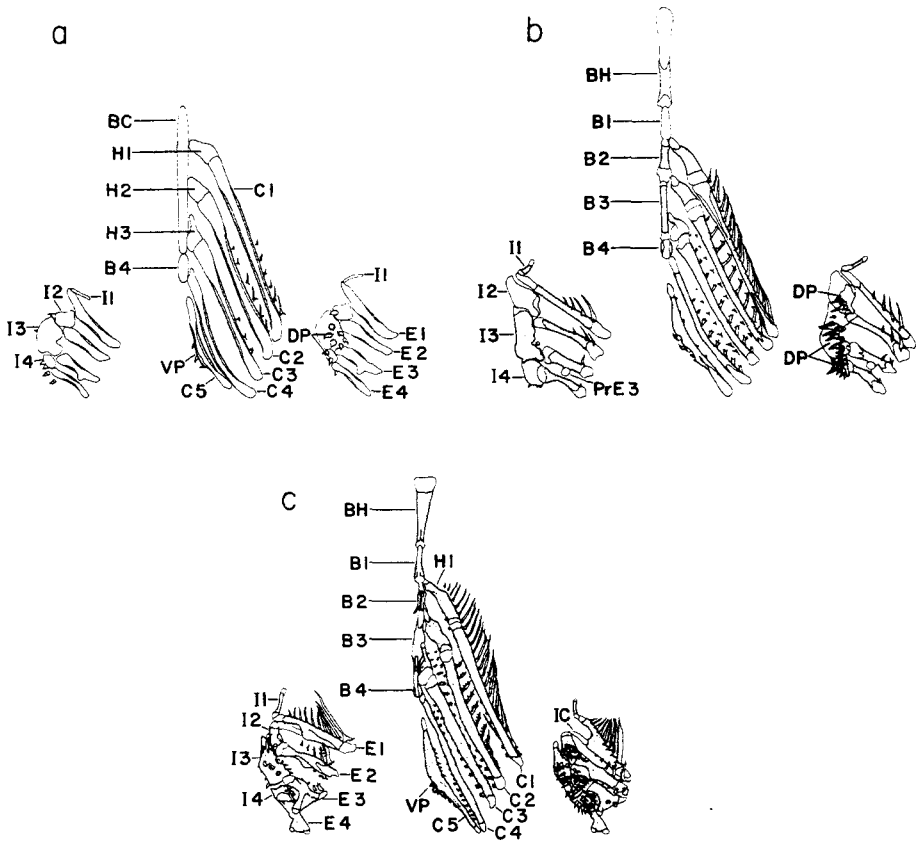

Figure 19. Development of the branchial arches of salema, *Xenistius californiensis*: a. 6.0 mm (SIO 91-135); b. 9.6 mm (SIO 91-135); c. 21.2 mm (SIO 62-356). White = cartilage; stippled = ossifying. Abbreviations are defined in Figure 8.

sequence of ossification (e.g., basibranchial 4 begins ossifying before hypobranchial 3 in salema, while the reverse is true for sargo), and salema acquires more gill rakers than sargo (Tables 3, 6).

Axial Skeleton (Figs. 20, 21; Tables 5, 6).—VERTEBRAL COLUMN (Fig. 20). Development of the neural and haemal pre- and postzygapophyses could not be tracked in the cleared and stained salema, since none were present in specimens 9.8 mm or smaller, but all were present in the next larger specimen (21.2 mm).

PLEURAL AND EPIPLEURAL RIBS. Salema acquires only 6–7 epipleural ribs, vs. 8–9 in sargo.

CAUDAL FIN (Fig. 21). Hypural 2 supports a single principal caudal ray through ca. 7 mm, but by ca. 9–10 mm the uppermost ray originally supported by hypural 1 shifts farther upward, to be supported jointly by hypurals 1 and 2. In comparison, hypural 2 of sargo originally supports two principal rays; the lowermost of these shifts downward to become jointly supported by hypurals 1 and 2. Like sargo, salema has only two radial cartilages in the lower caudal skeleton, but in contrast to sargo, salema has a small, separate radial cartilage adjacent to hypural 5 by 21.2 mm. Uroneural development could not be tracked in sargo; in salema the

Table 6. Counts of fin spines and rays, vertebrae, ribs, gill rakers (outer arch: counts are given as epibranchial, and hypobranchial + certobranchial; one raker at the ceratobranchial-epibranchial articulation is counted with the ceratobranchial rakers), and branchiostegal rays in *Xenistius californiensis*. Specimens between dashed lines are undergoing notochord flexion; those below the solid lines are juveniles

	Fin rays							Ribs			
Length (mm)	1°C	2°C	D	A	P_1	P_2	Vertebrae	Pleural	Epi-pleural	Gill rakers	Branchi-ostegal rays
2.7											
3.9	3+3										5
4.1	2+2										4
4.2	5+5										4
4.3	3+3									0+2	6
4.4	3+3						2			0+2	5
4.4	4+4									0+3	6
4.9	7+6									0+4	6
5.3	9+8						10+9			0+8	7
5.5	8+8						10+10			0+8	7
5.7	9+8						10+5			0+7L,8R	7
5.7*	9+8	0+1	12	10			10+14			1+9	7
5.8	9+8		3	3			10+5			0+7L,8R	7
5.9	9+8	0+1	7	5			10+7			0+8	7
6.0	7+7						10+2			0+6	6
6.0	9+8		9	8			10+7			0+7L,8R	7
6.3	9+8	0+1	11	11			10+12			0+9	7
6.3	9+8	0+1	10	10			10+12			0+10	7
6.5	9+8	0+1	I,13	I,12	2		10+16			1+13	7
6.8	9+8	0+2	—	11			10+14			1+10	7
7.4	9+8	1+1	II,12	I,12	4		10+16			2+13	7
7.8	9+8	2+3	IV+II,12	I,11	7	I,1	10+16			2+13	7
9.6	9+8	5+5	XII,12	II,12	13	I,5	10+16	4	3	4+16	7
21.2	9+8	13+12	XII,13	III,11	18	I,5	10+16	8	6	—	7
24.1	9+8	13+12	XI,14	II,12	I,17	I,5	10+16	8	7	12+26	7

* Postflexion specimen, probably shrunken.

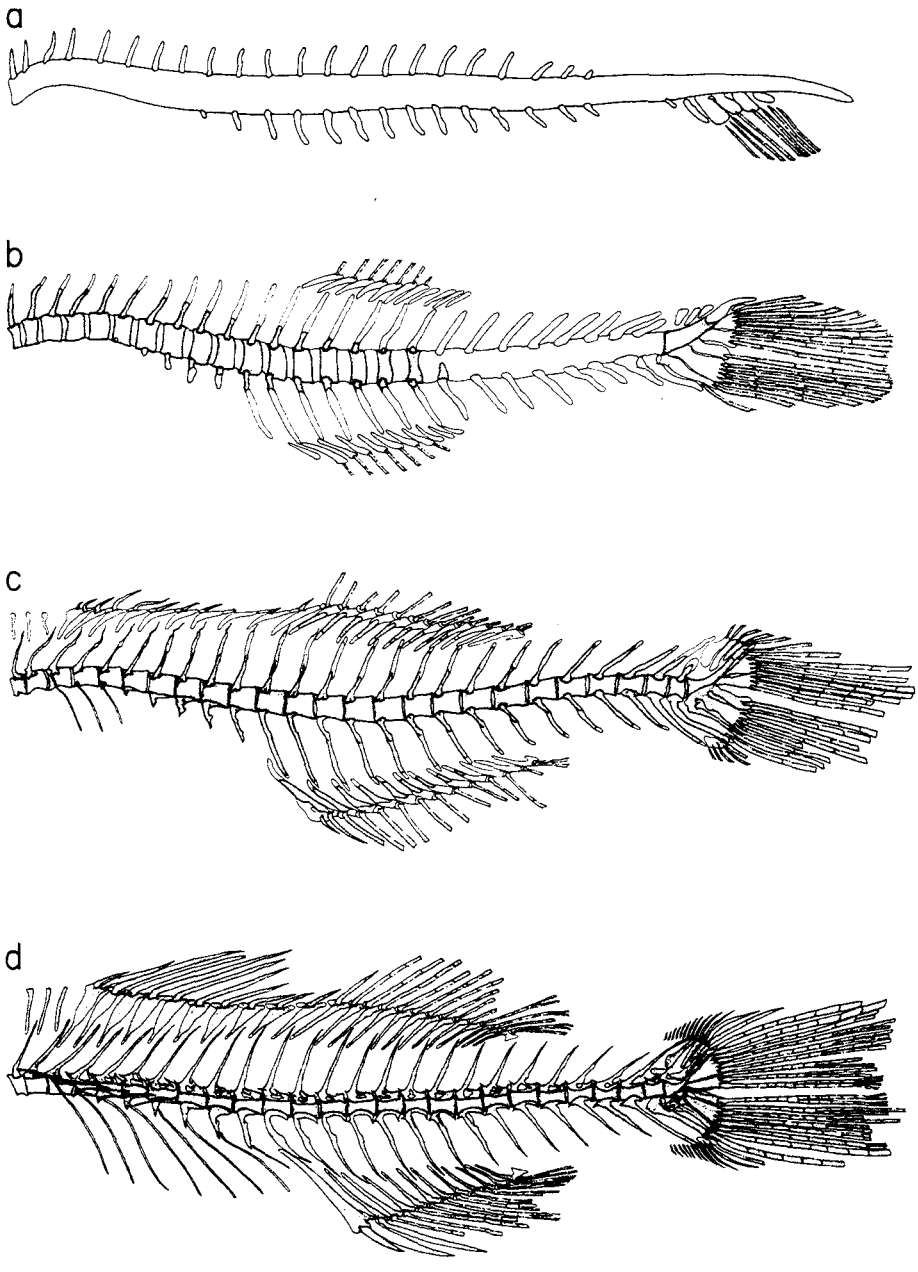

Figure 20. Development of the axial skeleton of salema, *Xenistius californiensis*: a. 4.4 mm (SIO 91-135); b. 5.9 mm (SIO 91-135); c. 9.6 mm (SIO 91-135); d. 21.2 mm (SIO 62-356). White = cartilage; stippled = ossifying.

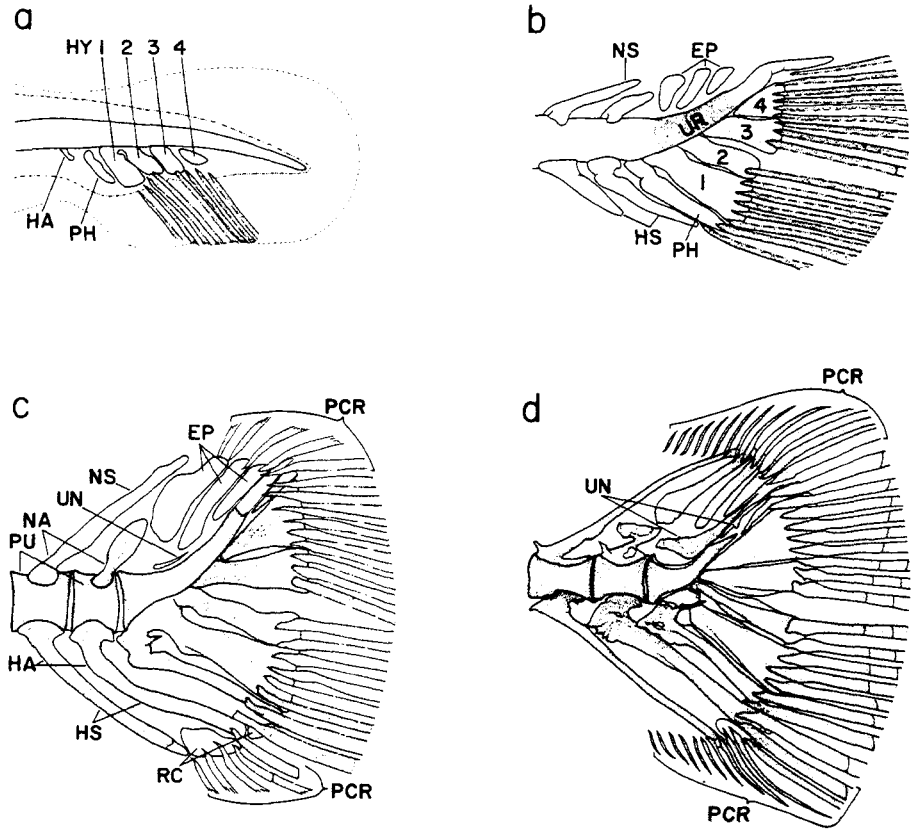

Figure 21. Development of the caudal skeleton of salema, *Xenistius californiensis*: a. 4.4 mm (SIO 91-135); b. 5.9 mm (SIO 91-135); c. 9.6 mm (SIO 91-135); d. 21.2 mm (SIO 62-356). White = cartilage; stippled = ossifying. Abbreviations are defined in Figure 10.

anterior pair begins ossifying first, by 9.6 mm, and both pairs are well developed by 21.2 mm.

Dorsal and Anal Fins. Cartilaginous pterygiophores of the middle dorsal and anal fin rays are the first elements to form, at ca. 5 mm, with the rays following at ca. 5.5 mm (Tables 5, 6). It seems likely that the first anal pterygiophore (which supports the first two spines) results from the fusion of two cartilages: separate cartilages were not seen in any specimen, but in the 7.4 mm specimen a slender anterior section of cartilage is attached only at its proximal end to the remainder of the pterygiophore. The first dorsal pterygiophore (which supports the first two dorsal spines) does originate as two separate cartilages: both are visible and clearly separate in the 7.4 mm specimen. The second and third anal spines develop from rays, as in *Anisotremus virginicus* (Potthoff et al., 1984).

Pectoral and Pelvic Girdle (Fig. 22; Tables 5, 6).—The coracoscapular cartilage is visible sooner, and the pectoral proximal radials may develop sooner, but ossify later, in salema than in sargo (Tables 2, 5). The first cleavage of the cartilaginous pectoral blade was visible in a 4.4 mm specimen (it could not be determined

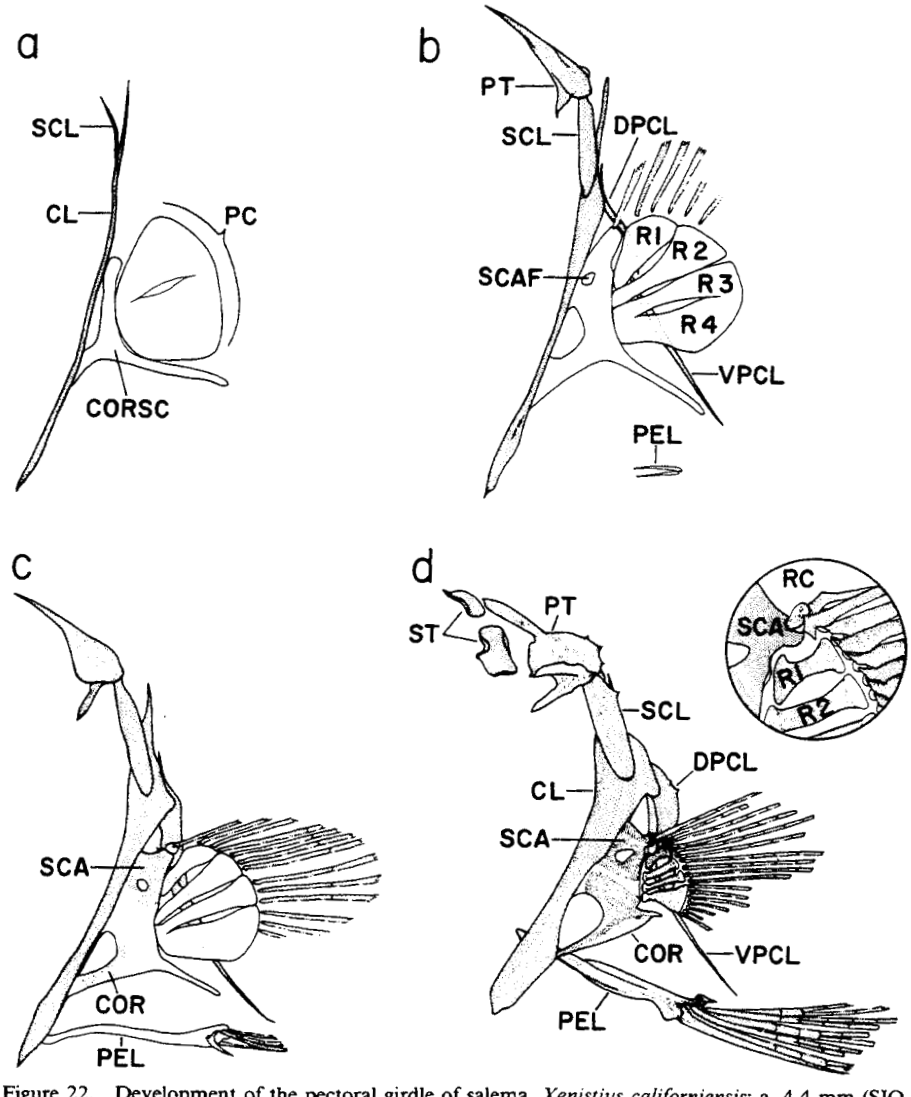

Figure 22. Development of the pectoral girdle of salema, *Xenistius californiensis*: a. 4.4 mm (SIO 91-135); b. 7.4 mm (SIO 91-135); c. 9.6 mm (SIO 91-135); d. 21.2 mm (SIO 62-356). White = cartilage; stippled = ossifying. Abbreviations are defined in Figure 11.

whether cleavages were present in any smaller specimen), and all three cleavages were visible by ca. 5 mm. It could not be determined when proximal radial ossification begins: none were ossifying through 9.6 mm, but all were ossifying in the 21.2 m specimen (Fig. 22).

Identification

Haemulid larvae resemble the lightly-pigmented larvae of many percoid families (Johnson, 1984; Leis and Rennis, 1983; Watson, 1983). However, in the

waters off California and northern Baja California, only larvae of the sciaenid, *Seriphus politus,* might be confused with larval sargo and salema. Confusion here can occur only for preflexion and early flexion-stage specimens; very small or damaged specimens cannot always be distinguished. Larval *S. politus* tend to be slightly deeper-bodied (depth 23–29% of SL) than sargo (19–28%) or salema (15–26%), and have a smaller eye (7–9% of SL, mean 8% during the preflexion stage, vs. 8–11%, mean 10% during the preflexion stage, for both sargo and salema). Pigmentation usually allows separation of the early larvae as well. The most reliable pigment character is the melanophore series along the ventral margin of the tail. Preflexion-stage sargo and salema both have series of evenly-spaced melanophores of approximately uniform size, while preflexion-stage *S. politus* have a series of approximately evenly-spaced and more-or-less uniform size melanophores along most of the tail, but much smaller, irregularly-spaced melanophores along the last 2–3 myomeres and under the notochord tip. The number of melanophores along the ventral margin of the tail subsequently decreases slightly in sargo and salema, but declines substantially in *S. politus* (usually <10 by mid-way through notochord flexion). Later, the higher dorsal and anal fin ray counts of *S. politus* allow easy and positive separation.

South of Bahia Sebastian Vizcaino, Baja California, positive identification of larval sargo and salema may be more difficult. In these waters, larval gerreids (*Eucinostomus* spp.), sparids (*Calamus brachysomus*), and several haemulid species might be confused with sargo and/or salema. Larval *C. brachysomus* are undescribed, but both they and larval *Eucinostomus* spp. should be separable from larval sargo and salema by myomere counts: the described sparid and gerreid larvae have 24 myomeres (rarely 25 in *Eucinostomus* spp.) vs. 26 (rarely 25) for sargo and salema. Larval *Eucinostomus* spp. also can be distinguished from sargo and salema by pigment characters and preopercular spines. *Eucinostomus* spp. develop external pigment (usually a pair of melanophores) over the midbrain at about the beginning of hypural development, while neither sargo nor salema acquire external pigment in this region until near the end of larval development. Throughout larval development the first 1–5 postanal myomeres (usually the first 2 or 3) are unpigmented in *Eucinostomus* spp.; during the preflexion stage (usually later, as well) both sargo and salema have pigment on all but the first one or two postanal myomeres. *Eucinostomus* spp. acquire dorsal pigment along the bases of the soft dorsal rays by ca. 7–8 mm while similar pigment first develops at a much larger size (>12 mm) in sargo and salema. Finally, *Eucinostomus* spp. have no, or at most very small (postflexion stage only), preopercular spines in contrast to the easily discernable preopercular spines of all but the smallest sargo and salema.

Larval development has not been described for any of the haemulid species that are sympatric with sargo and salema off southern Baja California and it is unknown how any of these, except *Orthopristis,* might be distinguished from larval sargo or salema. Larval *Orthopristis reddingi* have smaller, and fewer, spines on the opercular series bones and tend to have a longer preanal length than either sargo or salema (mean 53% of SL, vs. $<50\%$ for sargo and $\leq 52\%$ for salema).

It can be difficult to distinguish larval sargo from salema prior to notochord flexion, but older specimens usually are easily separable. Many pigment and morphometric characters differ somewhat between the two species, but do not reliably distinguish individual specimens during the preflexion stage. However, two pigment characters do consistently differ between sargo and salema: sargo usually have pigment on the peritoneum just anterior to the liver (present in 87% of preflexion sargo, absent in preflexion salema), while salema nearly always have

a melanophore under the anterior hindbrain (present in 90% of salema, and in 4% of preflexion sargo). The presence or absence of anterior peritoneal pigment usually allows species identification through notochord flexion; during this stage sargo becomes noticeably deeper-bodied as well (mean depth 25% of SL vs. 23% for salema). Morphometric differences (body depth, pre-anus length), pigmentation (especially the midbrain pigment of salema), and dorsal soft ray counts (14–15 for sargo, 12–13 for salema) allow easy separation of postflexion-stage specimens.

Discussion

The purpose of this discussion is to briefly compare the larval development of sargo and salema with development in other haemulids. Larvae of the two haemulid subfamilies, Haemulinae and Plectorhynchinae, apparently differ both in pigmentation and morphology. Haemulines are lightly pigmented through most of the larval stage, but develop a pattern of two or more longitudinal stripes along the upper half of the body early in the juvenile stage (Courtenay, 1961; Hong, 1977; Leis and Rennis, 1983; Lindeman, 1986; Potthoff et al., 1984; Saksena and Richards, 1975; Watson, 1983). Plectorhynchines also are relatively lightly pigmented early in larval development, but may become moderately to heavily pigmented subsequently (Kobayashi and Iwamoto, 1984; Leis and Rennis, 1983); *Parapristipoma* is an exception in that it remains lightly pigmented (Okiyama, 1988), like the haemulines.

Larval haemulines are relatively slender (Leis and Rennis, 1983; Lindeman, 1986; Potthoff et al., 1984; Saksena and Richards, 1975; Watson, 1983), while larval plectorhynchines, except *Parapristipoma,* tend to be somewhat deeper-bodied (Leis and Rennis, 1983; Kobayashi and Iwamoto, 1984; Okiyama, 1988). Larval sargo and salema are typical haemulines both in pigmentation and morphology, except that sargo, as well as *Anisotremus virginicus* (Potthoff et al., 1984), is somewhat deeper-bodied than the other described haemulines.

The few published descriptions of skeletal development in Haemulidae that are available for comparison with development in sargo and salema are of haemulines: Potthoff et al. (1984) described development of *Anisotremus virginicus,* Lindeman (1986) described development of *Haemulon flavolineatum* from ca. 6 mm, and Saksena and Richards (1975) described ossification in *H. plumieri.* In addition to these descriptions, seven cleared and alizarin-stained *Orthopristis chrysoptera* (3.4–13.0 mm: preflexion through late postflexion) were examined in the present study.

Based on these few species, it appears that skeletal development differs little among the Haemulinae; differences between species are largely limited to small differences in the size at which developmental events occur (Table 7), small differences in the shapes of some bones, and differences in the number of elements in some skeletal structures (Table 8). Very few consistent intergeneric differences are discernable, although it appears that there may be gradients in larval size at onset of ossification, and in the number and size of spines on the opercular series bones and pectoral girdle.

Although the order in which bones ossify differs little among the Haemulinae, ossification of most bones begins at a somewhat smaller larval size in *Anisotremus* and *Xenistius* than in *Orthopristis,* which in turn may begin ossifying at a slightly smaller size than *Haemulon* (Table 7). Ossification in *Anisotremus* may be slightly precocious relative to that in *Xenistius.*

Orthopristis apparently has the smallest, and least numerous spines on the opercular bone series among the Haemulinae (Table 8; Lindeman, 1986). *Xenistius*

Table 7. Larval size at the beginning of ossification of selected skeletal elements in Haemulinae. Sources of information are: *Anisotremus davidsonii* (this study), *A. virginicus* (Potthoff et al., 1984), *Haemulon flavolineatum* (Lindeman, 1986), *H. plumieri* (Saksena and Richards, 1975), *Orthopristis chrysoptera* (this study), *Xenistius californiensis* (this study)

	Approximate size at beginning of ossification (mm)					
Structure	*Anisotremus davidsonii*	*A. virginicus*	*Haemulon flavolineatum*	*H. plumieri*	*Orthopristis chrysoptera*	*Xenistius californiensis*
Neurocranium						
Frontal	5	–	11–13	≤10	7	5.5
Parietal	6.6	–	11–13	≤10	7	7
Supraoccipital crest	8.5–9	–	19–20	≤10	12	7–7.5
Vomer	6.6	–	–	4.6	6.3	5
Jaws and suspensorium						
Dentary	≤2.9	–	≤6.2	4.6	≤3.4	3.9
Premaxillary	≤2.9	–	≤6.2	5.8	≤3.4	3.9
Quadrate	4.2	–	≤6.2	4.6	5.1	4.9
Symplectic	3.9	–	>6.2, ≤9–10	4.6	5.1	4.4
Opercular bones						
Interopercular	4.2	5.7	≤6.2	5.8	6.3	4.9
Opercular	≤2.9	5.7	≤6.2	8.2	5.1	4.4
Preopercular	≤2.9	3.5	≤6.2	4.6	5.1	4.4
Subopercular	4.2	5.7	≤6.2	5.8	6.3	4.9
Hyoid arch						
Branchiostegal	3.9	3.5	≤6.2	4.6	≤3.4	3.9
Ceratohyal	3.9	7.5	≤6.2	5.8	5.1	4.4
Epihyal	4.2	7.5	≤6.2	5.8	5.1	4.4
Hypohyal	4.6–5.7	7.5–10	–	5.8	7	4.9–6
Branchial arch						
Basibranchial	5.5	5.7	>6.2	5.8	7	6
Ceratobranchial	4.2	5.7	>6.2	5.8	6.3	4.9
Epibranchial	4.2	5.7	>6.2	5.8	6.3	4.9
Gill rakers	4.3	3.8	≤6.3	5.8	6.3	4.3
Hypobranchial	5.5	5.7	>6.2	5.8	≤12	6
Axial skeleton						
Vertebral centra	4.5	>4.3, ≤5.7	8.5–9	9.2	6.3	4.4

has more preopercular spines than *Anisotremus* or *Haemulon,* but fewer interopercular spines than *Anisotremus* (Table 8). All of these spines are about the same size as the corresponding spines in *Anisotremus* and *Haemulon.* In addition to the opercular series spines, *Anisotremus* and *Xenistius* acquire one or two small supracleithral spines and about three small posttemporal spines. These are lacking in *Orthopristis,* and it is unclear whether *Haemulon* has them or not. *Pomadasys* is distinctly spinier, with several small to moderate spines each on the preopercular margins and on the interopercular and/or subopercular margins, moderate supracleithral and/or posttemporal spines, and small supraocular spines (Leis and Rennis, 1983). *Conodon* is highly ornamented, with several moderate to large preopercular spines, interopercular and/or subopercular spines, supraocular and other head spines, and apparently with cleithral spines in addition to supracleithral and posttemporal spines (Heemstra, 1974; Johnson, 1984). The described plectorhynchines fall between *Pomadasys* and *Conodon* in this series, except *Parapristipoma,* which is more like *Anisotremus* and *Xenistius* (Kobayashi and Iwamoto, 1984; Leis and Rennis, 1983; Okiyama, 1988).

Table 8. Counts of selected skeletal elements acquired in larvae or young juveniles of Haemulinae. Gill raker counts refer to the outer arch, and are given as hypobranchial + ceratobranchial, and epibranchial rakers. The number of caudal distal radial cartilages refers to the number in the ventral caudal skeleton. Sources of information are: *Anisotremus davidsonii* (this study), *A. virginicus* (Potthoff et al., 1984), *Haemulon flavolineatum* (Lindeman, 1986), *H. plumieri* (Saksena and Richards, 1975), *Orthopristis chrysoptera* (this study), *Xenistius californiensis* (this study)

	Counts					
Structure	*Anisotremus davidsonii*	*A. virginicus*	*Haemulon flavolineatum*	*H. plumieri*	*Orthopristis chrysoptera*	*Xenistius californiensis*
Gillrakers	13–16+9–12	14–16+7–11	13–15+9–10	15+10	12+4–5	26+12
Interopercular spines	4–5	2–4	—	1–2	0	1
Preopercular spines						
Interior shelf	7–8	10–12	ca. 7–9	ca. 5–10	4–5	14–15
Exterior shelf	2–3	2–3	ca. 4	ca. 3	0–3	3–4
Subopercular spines	1	1–3	—	1–2	0	1
Vertebrae	10+16	10+16	10+16	10+15–16	10+16	10+16
Pleural ribs	8	8	8	—	8	8
Epipleural ribs	8–9	11–12	11	>10	≥6	6–7
Dorsal fin rays	XI,14–15	XII–XIII,15–16	X–XII,14–15	XII,15–16	XII,15–17	XI–XII,12–14
Anal fin rays	III,9–10	II,11–12 (III,10–11)	II,9(III,8)	II,10 (III,9)	II,14–15 (III,13–14)	II–III,11–12 (III,11–12)
Pectoral fin rays	17–19	16–17	14–16	16–17	17–19	17–18
Procurrent caudal rays	12–14+11–13	13+12	10–12+11–12	10–12+10–12	13+12	13+12
Caudal distal radial cartilages	2	3	2	—	2	2

Vomerine teeth are present in larval *Anisotremus davidsonii* and *Orthopristis chrysoptera,* but absent in *Xenistius californiensis.* The presence or absence of vomerine teeth was not noted in the studies of other species. Most haemulids lack vomerine teeth as adults (Johnson, 1980) and their presence in larvae might prove useful in examining relationships, once more is known of their occurrence in the various haemulid genera. Furthermore, the existence of gradients in the size at initiation of ossification and in the degree of head and pectoral girdle spination might also prove of value in examining phylogenetic relationships among the haemulid genera. However, the potential utility of these characters cannot be assessed until larval development within the family is much more fully documented.

Acknowledgments

This study was undertaken as part of a larger study of the ichthyoplankton off San Onofre, California, conducted by MEC Analytical Systems for the Marine Review Committee of the California Coastal Commission. The Marine Review Committee does not necessarily accept the results, findings, or conclusions stated herein. We wish to thank the many technicians at MEC Analytical Systems who spent long hours collecting and processing the plankton samples that provided the basis for this study. H. G. Moser reviewed an earlier draft of the manuscript and provided helpful comments. L. Prescott typed the manuscript.

Literature Cited

Ambrose, D. A., R. L. Charter, H. G. Moser and B. S. Earhart. 1988. Ichthyoplankton and station data for California Cooperative Oceanic Fisheries Investigations survey cruises in 1981. U.S. Dep. Commer., NOAA Tech. Memo., NOAA-TM-NMFS-SWFSC-112. 170 pp.

Barnett, A. M., A. E. Jahn, P. D. Sertic and W. Watson. 1984. Distribution of ichthyoplankton off San Onofre, California, and methods for sampling very shallow coastal waters. Fish. Bull., U.S. 82: 97–111.

Courtenay, W. R. 1961. Western Atlantic fishes of the genus *Haemulon* (Pomadaysidae): systematic status and juvenile pigmentation. Bull. Mar. Sci. Gulf Caribb. 11: 66–149.

Feder, H. M., C. H. Turner and C. Limbaugh. 1974. Observations on fishes associated with kelp beds in southern California. Calif. Dep. Fish Game, Fish Bull. 160: 1–144.

Heemstra, P. C. 1974. On the identity of certain eastern Pacific and Caribbean post-larval fishes (Perciformes) described by Henry Fowler. Proc. Acad. Nat. Sci. Phila. 126: 21–26.

Hong, S. L. 1977. Review of eastern Pacific *Haemulon* with notes on juvenile pigmentation. Copeia 1977: 493–501.

Johnson, G. D. 1980. The limits and relationships of the Lutjanidae and associated families. Bull. Scripps Inst. Oceanogr. 24. 114 pp.

———. 1984. Percoidei: development and relationships. Pages 464–498 *in* H. G. Moser, W. J. Richards, D. M. Cohen, M. P. Fahay, A. W. Kendall, Jr. and S. L. Richardson, eds. Ontogeny and systematics of fishes. Am. Soc. Ichthyol. Herpetol., Spec. Publ. No. 1.

Kobayashi, T. and T. Iwamoto. 1984. Early life history of the threebanded sweetlip, *Plectorhynchus cinctus.* Jap. J. Ichthyol. 30: 412–418.

Leis, J. M. and D. S. Rennis. 1983. The larvae of Indo-Pacific coral reef fishes. New South Wales Univ. Press, Sydney. 269 pp.

Lindeman, K. C. 1986. Development of larvae of the French grunt, *Haemulon flavolineatum,* and comparative development of twelve species of western Atlantic *Haemulon* (Percoidei, Haemulidae). Bull. Mar. Sci. 39: 673–716.

Miller, D. J. and R. N. Lea. 1972. Guide to the coastal marine fishes of California. Calif. Dep. Fish Game, Fish Bull. 157: 1–235.

Okiyama, M., ed. 1988. An atlas of the early stage fishes in Japan. Tokai Univ. Press. 1154 pp.

Potthoff, T. 1984. Clearing and staining techniques. Pages 35–37 *in* H. G. Moser, W. J. Richards, D. M. Cohen, M. P. Fahay, A. W. Kendall, Jr. and S. L. Richardson, eds. Ontogeny and systematics of fishes. Am. Soc. Ichthyol. Herpetol., Spec. Publ. No. 1.

———, S. Kelley, M. Moe and F. Young. 1984. Description of porkfish larvae (*Anisotremus virginicus,* Haemulidae) and their osteological development. Bull. Mar. Sci. 34: 21–59.

Saksena, V. P. and W. J. Richards. 1975. Description of eggs and larvae of laboratory-reared white grunt, *Haemulon plumieri* (Lacepede) (Pisces, Pomadasyidae). Bull. Mar. Sci. 25: 523–536.

Sandknop, E. M., R. L. Charter, H. G. Moser, C. A. Meyer and A. E. Hays. 1988. Ichthyoplankton and station data for California Cooperative Oceanic Fisheries Investigations survey cruises in 1978. U.S. Dep. Commer., NOAA Tech. Memo., NOAA-TM-NMFS-SWFSC-111. 216 pp.

Stevens, E. G. and H. G. Moser. 1982. Observations on the early life history of the mussel blenny, *Hypsoblennius jenkinsi,* and the bay blenny, *Hypsoblennius gentilis,* from specimens reared in the laboratory. Calif. Coop. Oceanic Fish. Invest. Rep. 23: 269–275.

———, R. L. Charter, H. G. Moser and C. A. Meyer. 1990. Ichthyoplankton and station data for California Cooperative Oceanic Fisheries Investigations survey cruises in 1984. U.S. Dep. Commer., NOAA Tech. Memo., NOAA-TM-NMFS-SWFSC-141. 157 pp.

Walker, B. W., R. R. Whitney and G. W. Barlow. 1961. The fishes of the Salton Sea. Pages 77–92 *in* B. W. Walker, ed. The ecology of the Salton Sea, California, in relation to the sportfishery. Calif. Dep. Fish Game, Fish Bull. 113.

Walker, H. J., Jr., W. Watson and A. M. Barnett. 1987. Seasonal occurrence of larval fishes in the nearshore Southern California Bight off San Onofre, California. Estuarine, Coastal Shelf Sci. 25: 91–109.

Watson, W. 1983. Redescription of larvae of the pigfish, *Orthopristis chrysoptera* Linnaeus (Pisces, Haemulidae). Fish. Bull., U.S. 81: 847–854.

DATE ACCEPTED: January 29, 1992.

ADDRESSES: *(W.W.) NOAA National Marine Fisheries Service, Southwest Fisheries Science Center, P.O. Box 271, La Jolla, California 92038-0271; (H.J.W.) Scripps Institution of Oceanography, Marine Vertebrates Collection, University of California, San Diego, 0208, La Jolla, California 92093-0208.*